FLOWERING LOCUS T3 Controls Spikelet Initiation But Not Floral Development[1][OPEN]

Muhammad Aman Mulki,[a,b] Xiaojing Bi,[a] and Maria von Korff[a,b,c,2,3]

[a]Max Planck Institute for Plant Breeding Research, 50829 Cologne, Germany
[b]Institute of Plant Genetics, Heinrich-Heine-University, 40225 Düsseldorf, Germany
[c]Cluster of Excellence on Plant Sciences "From Complex Traits towards Synthetic Modules" 40225 Düsseldorf, Germany

ORCID IDs: 0000-0003-3511-537X (M.A.M.); 0000-0003-2240-1246 (X.B.); 0000-0002-6816-586X (M.v.K.)

In many angiosperm plants, *FLOWERING LOCUS T* (*FT*)-like genes have duplicated and functionally diverged to control different reproductive traits or stages. Barley (*Hordeum vulgare*) carries several *FT*-like genes, the functions of which are not well understood. We characterized the role of HvFT3 in the vegetative and reproductive development of barley. Overexpression of *HvFT3* accelerated the initiation of spikelet primordia and the early reproductive development of spring barley independently of the photoperiod. However, *HvFT3* overexpression did not accelerate floral development, and inflorescences aborted under short days, suggesting that HvFT3 controls spikelet initiation but not floral development. Analysis of a nonfunctional *HvFT3* allele supported the specific effects of this gene on spikelet initiation independent of the photoperiod. HvFT3 caused the upregulation of the winter and spring alleles of the vernalization gene *VERNALIZATION1* (*VRN-H1*) in nonvernalized plants and was therefore dominant over the repressive effects of the vernalization pathway. Global transcriptome analysis in developing main shoot apices of the transgenic lines showed that HvFT3 modified the expression of genes involved in hormone synthesis and response, of floral homeotic genes, and of barley row-type genes *SIX-ROWED-SPIKE1* (*VRS1*), *SIX-ROWED-SPIKE4* (*VRS4*), and *INTERMEDIUM C*. Understanding the specific functions of individual *FT*-like genes will allow modification of individual phases of preanthesis development and thereby adaptation to different environments and improved yield.

In most flowering plants, the transition from vegetative to reproductive development is triggered by a variety of environmental and endogenous cues (Boss et al., 2004; Michaels et al., 2005; Andrés and Coupland, 2012). The perception and integration of these cues ensure that floral transition is coordinated with favorable environmental conditions. In the model plant Arabidopsis (*Arabidopsis thaliana*), the photoperiod, vernalization, gibberellin, and the autonomous pathways have been defined as the main genetic pathways that regulate floral transition (Mouradov et al., 2002). The four pathways converge on a small set of genes known as the floral pathway integrator genes (Araki, 2001; Simpson and Dean, 2002). An important floral integrator gene is *FLOWERING LOCUS T* (*FT*), the product of which exhibits similarities to phosphatidylethanolamine-binding proteins and to Raf kinase inhibitor proteins (Kardailsky et al., 1999; Kobayashi et al., 1999). Under long day (LD) conditions, *FT* expression is induced in the leaves, and the FT protein moves to the shoot apical meristem (SAM) where it interacts with the bZIP transcription factor FLOWERING LOCUS D to activate floral meristem identity genes and the transition to flowering (Abe et al., 2005; Wigge et al., 2005; Corbesier et al., 2007).

The family of *FT*-like genes has expanded by gene duplications occurring independently in nearly all modern angiosperm lineages. The emergence of *FT*-like genes coincided with the evolution of flowering plants, and the potential of *FT*-like genes to promote floral transition seems conserved in angiosperms (Ballerini and Kramer, 2011). A few reports suggest that gene duplication was followed by diversification of *FT* functions within and between species. For example, in perennial poplar (*Populus* spp.), *FT* paralogs (*FT1*) and *FLOWERING LOCUS T2* (*FT2*) have functionally diverged to coordinate the repeated cycles of vegetative and reproductive growth (Hsu et al., 2011). The basis for functional differentiation between *FT*-like genes appears to be controlled by expression pattern shifts, changes in proteins, and divergence in gene regulatory networks (Hsu et al., 2011). However, the role of different *FT* paralogs within most flowering species is as yet undescribed.

[1]This research was funded by the German Cluster of Excellence on Plant Sciences (CEPLAS) EXC1028, the Priority Programme (SPP1530 Flowering time control: from natural variation to crop improvement), and the Max Planck Society. M.A.M. received a fellowship from the DAAD (German Academic Exchange Service). X.B. received a fellowship from the CSC (Chinese Scholarship Council).

[2]Author for contact: korff@mpipz.mpg.de.
[3]Senior author.

The author responsible for distribution of materials integral to the findings presented in this article in accordance with the policy described in the Instructions for Authors (www.plantphysiol.org) is: Maria von Korff (korff@mpipz.mpg.de).

M.A.M. and M.v.K. conceived and designed the experiments; M.A.M. conducted all experiments, and M.A.M. and X.B. analyzed the data; M.A.M, X.B., and M.K wrote the manuscript.

[OPEN]Articles can be viewed without a subscription.
www.plantphysiol.org/cgi/doi/10.1104/pp.18.00236

Genomes of cereal monocots are characterized by a large number of *FT*-like genes, i.e. wheat (*Triticum aestivum*) and barley (*Hordeum vulgare*) genomes each contain 12 *FT* paralogs (Halliwell et al., 2016), whereas 13 and 15 *FT*-like genes have been identified in rice (*Oryza sativa*) and maize (*Zea mays*), respectively (Chardon and Damerval, 2005; Danilevskaya et al., 2008). Functional diversification of *FT*-like genes has been demonstrated in rice, where *HEADING DATE3a* induces floral transition under inductive short day (SD) conditions, whereas its closest homolog, *Rice FT1* (*RFT1*), acts as the floral activator under LD conditions (Kojima et al., 2002; Hayama et al., 2003; Komiya et al., 2008, 2009). In both wheat and barley, *FT1* is the candidate gene for *VERNALIZATION3* (*VRN3*), which promotes flowering under LDs (Yan et al., 2006). In contrast, *HvFT3* was postulated as the candidate gene for the *PHOTOPERIOD RESPONSE2* (*Ppd-H2*) locus, which promotes reproductive development under SDs (Laurie et al., 1995; Faure et al., 2007). In barley, two alleles of *HvFT3* have been described; the dominant functional allele is prevalent in spring barley and winter barley from southern European cultivation areas, whereas the recessive nonfunctional allele with a large deletion in the transcribed coding region is typical for northern European winter barley (Kikuchi et al., 2009; Casao et al., 2011a, 2011b). Casao et al. (2011b) showed that the wild-type *HvFT3* allele promotes flowering of winter cultivars under noninductive conditions, i.e. under SDs or in plants that have not satisfied their vernalization requirement.

In barley, vernalization requirement is determined by the interaction of two genes, *VRN-H2*, a strong inhibitor of *HvFT1* and hence flowering under LD conditions, and *VRN-H1*. *VRN-H1*, an *APETALA1* (*AP1*)/*CAULIFLOWER*/*FRUITFULL* (*FUL*)-like MADS box transcription factor, is upregulated during vernalization and represses *VRN-H2* to release *HvFT1* expression (Yan et al., 2003, 2004). A deletion of the *VRN-H2* locus and deletions in the regulatory regions of the first intron of *VRN-H1* induce the expression of *HvFT1* independent of vernalization and cause a spring growth habit (Hemming et al., 2009; Rollins et al., 2013). In spring or vernalized winter barley, LDs strongly promote flowering, whereas SDs delay reproductive development. Flowering under LDs is controlled by the major photoperiod response gene *Ppd-H1*, which upregulates *HvFT1* in the leaf under LDs (Turner et al., 2005). A natural mutation in the conserved CCT domain of *Ppd-H1* prevalent in spring barley causes a delay in the induction of *HvFT1* and later flowering under LDs (Turner et al., 2005; von Korff et al., 2006, 2010; Jones et al., 2008; Wang et al., 2010). In the leaf, *HvFT1* expression is correlated with the up-regulation of the barley MADS box (BM) genes *VRN-H1*, *HvBM3/FUL2*, and *HvBM8/FUL3* and successful inflorescence development and flowering (Hemming et al., 2008; Sasani et al., 2009; Digel et al., 2015; Ejaz and von Korff, 2017).

Reproductive development in temperate cereals can be divided into three major phases based on morphological changes of the shoot apex: leaf initiation (vegetative phase), spikelet initiation (early reproductive phase), and spike growth and floral development (late reproductive phase; Appleyard et al., 1982; Slafer and Rawson, 1994; González et al., 2002; Campoli and von Korff, 2014). Physiological studies of preanthesis development in barley and wheat show that vernalization controls flowering time, predominantly by reducing the duration of the vegetative phase (Griffiths et al., 1985; Roberts et al., 1988; González et al., 2002). Additionally, vernalization affects the late reproductive phase and floral development (González et al., 2002). In spring and vernalized winter barley, LDs shorten the vegetative phase but primarily accelerate the late reproductive phase of stem elongation and floral development (Roberts et al., 1988; Miralles and Richards, 2000; Digel et al., 2015, 2016). In spring barley, spikelet initiation occurs under both SDs and LDs whereas floral development depends on LDs and the expression of *HvFT1* (Digel et al., 2015). The regulation of *HvFT3* and its effects on spikelet initiation and floral development has not yet been examined.

By studying the effects of *HvFT3* overexpression and the natural deletion of *HvFT3* on reproductive development, we demonstrate that *HvFT3* specifically promotes spikelet initiation and accelerates the early reproductive phase under SD and LD conditions but does not promote floral development in barley. Analysis of gene expression revealed that *HvFT3* overexpression accelerates spikelet initiation through the down-regulation of putative floral repressors and the up-regulation of floral homeotic genes at the shoot apices of transgenic plants.

RESULTS

Overexpression of *HvFT3* Accelerated Flowering Time of Spring Barley under LD But not under SD Conditions

We investigated the effect of *HvFT3* on flowering time by ectopically overexpressing *HvFT3* in the spring variety Golden Promise (spring *VRN-H1*, spring *vrn-H2*, and reduced photoperiod sensitivity *ppd-H1*) and analyzing flowering time and development of the main shoot apex (MSA) under LDs and SDs. We scored flowering time in days from germination until heading where heading denotes the emergence of spike awns out of the sheath of the main shoot flag leaf (Zadoks stage 49; Zadoks et al., 1974). Under LDs, the constitutive overexpression of *HvFT3* significantly accelerated flowering. The five independent transgenic *Ubi::HvFT3* lines required 52 to 56 d to flower, whereas Golden Promise and the null segregants flowered 66 d after germination (DAG; Fig. 1A). In contrast, none of the plants flowered before 120 DAG, when the

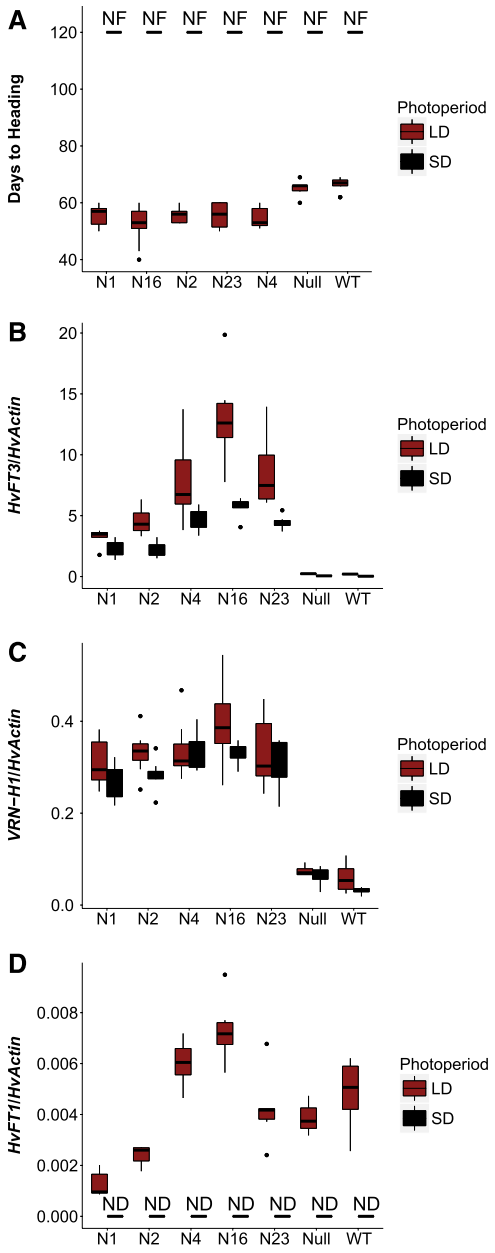

Figure 1. Flowering time and gene expression levels in *Ubi::HvFT3* transgenic lines under long-day and short-day conditions. Flowering time and expression levels of *HvFT3*, *VRN-H1*, and *HvFT1* were estimated in *Ubi::HvFT3* transgenic lines (N1, N2, N4, N16, and N23), a null segregant line (Null), and Golden Promise (wild type [WT]) under long day (LD; 16 h light, red) and short day (SD; 8 h light, black) conditions. Each column represents the average (A) flowering time, (B) *HvFT3* expression levels, (C) *VRN-H1* expression levels, and (D) *HvFT1* expression levels. Flowering time was measured in days from germination until heading. For A, B, C, and D, four to 15 plants were used as biological replicates. Error bars, standard deviation. Expression analysis was performed on leaf samples collected 2 h before the end of the light period at day 5 after germination. Expression values were normalized to *HvActin*. NF, Did not flower; ND, not detected.

experiment was stopped, under SDs (Fig. 1A). Under both photoperiods, however, *HvFT3* expression levels were significantly increased in the transgenic families compared to the control lines (Fig. 1B; Supplemental Fig. S1). Expression levels of *VRN-H1* were also significantly higher in the presence of the transgene under both photoperiods (Fig. 1C). *HvFT1* was only expressed under LDs but not SDs in the transgenic and wild-type lines. Overexpression of *HvFT3* did not affect *HvFT1* expression levels as these were not consistently altered in transgenic versus wild-type lines (Fig. 1D; Supplemental Fig. S1). We further examined whether variation at *Ppd-H1*, and thus *HvFT1* expression levels, affected *HvFT3* expression in wild-type plants. For this purpose, we evaluated *HvFT3* expression levels in Golden Promise (*ppd-H1*) and a derived introgression line with a wild-type *Ppd-H1* allele from the winter barley variety Igri over development under LDs and SDs. *HvFT3* expression levels were reduced in the introgression line with a wild-type *Ppd-H1* allele under LDs but not under SDs (Supplemental Fig. S2).

To further characterize the day-length-dependent effects of *Ubi::HvFT3*, we dissected the primary shoots of developing transgenic, null segregant and Golden Promise plants and determined differences in the timing of spikelet initiation and inflorescence development. We monitored phenotypic changes of the MSA and evaluated these according to the Waddington scale, a quantitative scale for barley and wheat development based on the morphogenesis of the shoot apex and carpels (Waddington et al., 1983; Fig. 2). The emergence of the first spikelet primordia on the shoot apex at the double-ridge stage (W1.5–W2.0) specifies a reproductive SAM. The first floral organ primordia differentiate and stem elongation initiates at the stamen primordium stage (W3.5). Anthesis and pollination of the most advanced floret occur at the last stage of the Waddington scale (W10.0).

Under LDs, early development of the MSA was strongly accelerated in *Ubi::HvFT3* compared to the null segregant and the wild-type lines (Fig. 2A). Apical meristems of the transgenic plants had already initiated spikelet primordia 4 DAG, whereas the control plants required 8 more days to reach the same stage. The transgenic plants developed stamen primordia (W3.5) 12 d earlier than the null segregants and Golden Promise. During further floral development, no additional acceleration in development of the transgenic compared to the control plants was observed. Eventually, the transgenic line flowered 44 DAG, while the null segregant and wild-type lines flowered 54 and 55 DAG, respectively. Under SDs, spikelet initiation (W2.0) occurred six DAG in *Ubi::HvFT3*, 22 d earlier than in null segregant and wild-type plants (Fig. 2B). Early reproductive development was further accelerated in the transgenic line as it developed stamen primordia (W3.5), on average 33 d earlier than in the two control genotypes. The MSA of the control plants failed to develop further than the pistil primordium stage (W4.0), whereas the MSA of *Ubi::HvFT3* plants reached

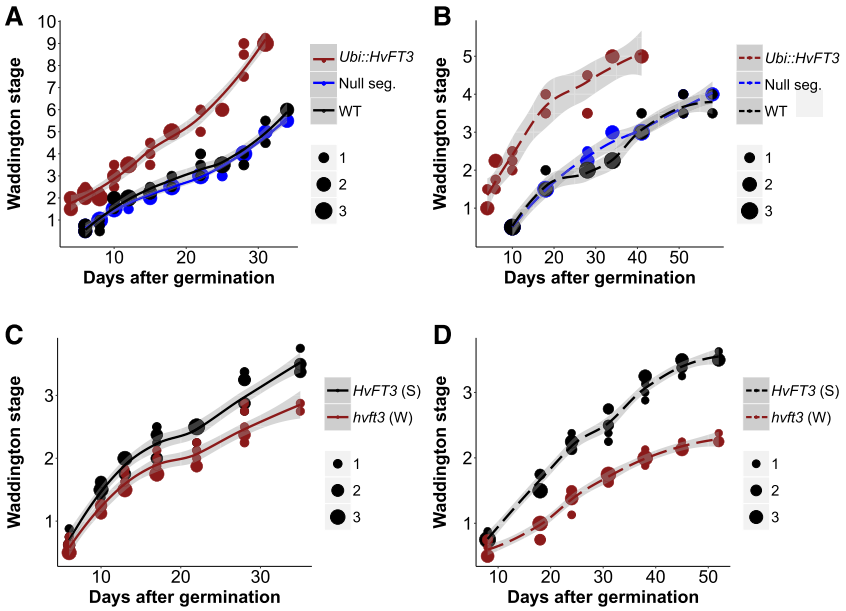

Figure 2. Effects of *HvFT3* on MSA development in spring barley under LDs and SDs. A and B, *Ubi::HvFT3* (red line), null segregant (dark blue), and wild-type (WT; black) plants were grown under (A) LD (16 h light) and (B) SD (8 h light), and meristem development was evaluated based on the Waddington scale. Two independent *Ubi::HvFT3* lines, N16 and N23, were used under LD and SD, respectively. Each value represents the average of 2 to 4 replicates. C and D, Meristem development of spring introgression lines carrying either the functional *HvFT3* (black) or the null *hvft3* allele (red) under (C) LD (13 h light) and (D) SD (8 h light). Meristem development was evaluated based on the Waddington scale. Each value represents the average of 4 to 6 replicates. The size of the dots shows the number of MSA with the same Waddington stage at a given time point. The shaded area indicates the 95% confidence interval (Loess smooth line) calculated using a polynomial regression model.

the carpel primordium stage (W5.0). None of the plants produced fertile florets and seeds under SDs.

Under both photoperiods, null segregants, wild-type plants, and the majority of transgenic plants formed normal shoot meristems that developed fertile flowers and set seeds under LDs (Supplemental Fig. S3A), while the MSA of approximately 20% of transgenic *Ubi::HvFT3* plants exhibited impaired development (Supplemental Fig. S3B). These meristems remained very small (Supplemental Fig. S1D), failed to develop floral primordia, and were prematurely aborted (Supplemental Fig. S3B). We also observed *Ubi::HvFT3* plants that developed floret primordia, but the architecture of their inflorescences was severely impaired, i.e. the shoot apices were not symmetrical, very short and compacted, and some inflorescences were branched.

We further analyzed the effect of natural variation at *HvFT3* on spikelet initiation and inflorescence development. We compared the MSA development of two sets of nontransgenic sister F_4 lines derived from the cross *Ubi::HvFT3* (Golden Promise) × Igri. These were isogenic for the vernalization genes (spring growth habit, *VRN-H1*/*vrn-H2*) and the mutated *ppd-H1* allele but segregating for the functional spring *HvFT3* allele from Golden Promise and the mutated nonfunctional allele *hvft3* introgressed from winter barley (Casao et al., 2011a, 2011b). The primary shoots of the two genotypes were dissected under SDs of 8 h light and LDs of 13 h light, which correspond to the photoperiod during early reproductive development of spring-sown barley plants in northern European cultivation areas. Under 13-h LDs, the MSA of *HvFT3* plants initiated spikelet primordia 4 d earlier and reached the stamen primordium stage 7 d earlier than *hvft3* plants (Fig. 2C). Genotypes with the functional *HvFT3* allele flowered on average in 84 DAG, significantly earlier than the *hvft3* introgression lines, which flowered on average 19 d later (some plants failed to flower by 120 DAG).

Under SD conditions, early development of the MSA was strongly enhanced in the presence of the spring *HvFT3* allele (Fig. 2D). Plants with the *HvFT3* allele reached the double-ridge stage (W2.0) 21 DAG and the stamen primordium stage (W3.5) 45 DAG, while lines carrying the *hvft3* allele initiated spikelet primordia 38 DAG but had not reached the glume primordia stage (W2.5) by 52 DAG. The inflorescences of *HvFT3* plants did not develop beyond the stamen primordium stage (W3.5), while *hvft3* plants stopped further development directly after spikelet initiation. Taken together, the natural variation in *HvFT3* specifically affected spikelet initiation and early reproductive growth of spring barley under SDs, as we also observed in the transgenic lines. Under 13 h LDs, *HvFT3* accelerated spikelet initiation and later inflorescence development.

We further explored the photoperiod- and stage-specific effects of *HvFT3* by overexpressing *HvFT3* in the Arabidopsis *ft10* mutant (Yoo et al., 2005). Flowering time was scored in three homozygous *35S::HvFT3* T_2 families, together with a mock family (*ft10* transformed with an empty vector), *35S::AtFT*, and the *ft10* mutant plants under LDs and SDs (Supplemental Fig. S4). The *35S::HvFT3* plants flowered with 18 to 28 leaves and 22 to 28 leaves under LDs and SDs, respectively, which was significantly earlier than the mock plants and the *ft10* mutant lines. These flowered with 33 to 35 leaves and >40 leaves under LDs and SDs, respectively. The *35S::AtFT* plants flowered with only five leaves under both photoperiods. Consequently, the overexpression of *HvFT3* accelerated flowering in Arabidopsis, but its effect was much smaller compared to that of *AtFT*.

Taken together, *HvFT3* promoted the initiation of spikelet primordia and accelerated early inflorescence development under both SDs and LDs as demonstrated by *HvFT3* overexpression and a natural *HvFT3* knockout line. However, both transgenic and wild-type plants headed and flowered only under LDs, i.e. the inflorescences were aborted under SDs. Overexpression of *HvFT3* was associated with a strong up-regulation of *VRN-H1*, but not *HvFT1* in the leaf under both tested photoperiods. In Arabidopsis, the overexpression of *HvFT3* accelerated flowering in the *ft10* mutant plants under both photoperiods. The photoperiod-dependent effect of *HvFT3* was consequently specific to barley, as overexpression of *HvFT3* in Arabidopsis accelerated flowering time under both photoperiods.

Overexpression of *HvFT3* Accelerated Flowering Time in Winter Barley

To analyze the genetic interaction of *HvFT3* with the vernalization genes *VRN-H1* and *VRN-H2* and the photoperiod response gene *Ppd-H1*, we examined flowering time and gene expression in an F_2 population developed by crossing *Ubi::HvFT3* in the background of Golden Promise to the winter variety Igri. Golden Promise carries a functional *HvFT3* gene, a natural mutation at *Ppd-H1* that reduces the response to LD (Turner et al., 2005), a deletion in the first regulatory intron of *VRN-H1* and a deletion of the *VRN-H2* locus. As a consequence, this genotype does not require vernalization and shows a reduced photoperiod response. In contrast, Igri carries a nonfunctional allele of *HvFT3*, the wild-type allele of *Ppd-H1*, and the winter alleles of *VRN-H1* and *VRN-H2*. Consequently, Igri requires vernalization to flower and shows a strong photoperiod response. The transgene *Ubi::HvFT3*, native *HvFT3*, *Ppd-H1*, *VRN-H1*, and *VRN-H2* were the main flowering time genes segregating in the generated F_2 population. To test whether overexpression of *HvFT3* can overcome the vernalization requirement, we scored flowering time of F_2 plants grown without vernalization under LDs.

Flowering time of *Ubi::HvFT3* × Igri F_2 lines varied between 25 and 111 d (Fig. 3A). The population exhibited strong transgressive segregation, as 70% of the lines flowered earlier than the transgenic parent, which required on average 47 d to flower. A few F_2 lines and the winter parent Igri did not flower before 120 DAG, when the experiment was stopped. The distribution of flowering time in the F_2 population was strongly skewed with the majority of lines flowering as early or earlier than the transgenic parent. Of the 166 F_2 lines from the *Ubi::HvFT3* Golden Promise × Igri population, 127 F_2 lines (76.51%) carried the transgene *Ubi::HvFT3* and 39 (23.49%) did not, which showed that the transgene segregated as a single insert.

Association of flowering time with the presence of *Ubi::HvFT3* and genetic variation at *Ppd-H1*, *VRN-H1*, and *VRN-H2* in the F_2 population showed that the transgene *Ubi::HvFT3* had the strongest effect on flowering time in the population (Supplemental Table S1). Transgenic F_2 lines flowered on average after 38 d, 37 d earlier than those without the transgene (Fig. 3B). *Ppd-H1* affected flowering time only in the transgenic subpopulation (Supplemental Fig. S5). In the presence of *Ubi::HvFT3*, lines with a photoperiod-responsive *Ppd-H1* allele flowered on average 9 d earlier than their siblings with the mutated *ppd-H1* allele. The allelic status of *Ppd-H1* had no significant effect on flowering in the nontransgenic F_2 lines, suggesting that in these lines the vernalization pathway was dominant over the photoperiod pathway. Allelic variation at *VRN-H2* and *VRN-H1* contributed to the overall observed variation in flowering time but did not affect the flowering time of the transgenic F_2 lines (Fig. 4A). Consequently, transgenic lines with the winter alleles *vrn-H1* and *VRN-H2* flowered even without vernalization. Overexpression of *HvFT3* was thus dominant over the vernalization pathway. By contrast, flowering of the nontransgenic F_2 lines was significantly delayed by the combination of the winter alleles of *VRN-H1* and *VRN-H2*. We could not evaluate the effects of the native *HvFT3* on flowering time in this population as only a limited number of genotypes (39) were not transgenic, and these carried additional background variation at *Ppd-H1*, *VRN-H1*, and *VRN-H2*, which masked the effect of the wild-type *HvFT3* locus on flowering time and gene expression.

To further characterize the molecular control of flowering time in the F_2 population under LDs, we analyzed the effects of *Ubi::HvFT3* and genetic variation at *Ppd-H1*, *VRN-H1*, and *VRN-H2* on expression levels of selected flowering time regulators. Flowering time exhibited the highest positive and negative correlations with expression levels of *VRN-H2* (0.80) and *VRN-H1* (−0.69; Supplemental Table S2), respectively. Flowering time also negatively correlated with expression of *HvFT3* (−0.48), *HvFT1* (−0.46), and *Ppd-H1* (−0.39). F_2 lines carrying the transgene had on average 650 times higher expression levels of *HvFT3* compared to their siblings with the wild-type gene only (Fig. 3C). The presence of the transgene was associated with a strong up-regulation of *VRN-H1* independently of allelic variation at *VRN-H1* (Fig. 4B). In contrast, the transgene caused a down-regulation of *VRN-H2* (Fig. 4C). Expression levels of *HvFT1* correlated negatively and positively with those of *VRN-H2* (−0.38) and *Ppd-H1* (0.39), but not with *HvFT3* or *VRN-H1* (Supplemental Table S2). Furthermore, *HvFT1* expression was mainly controlled by the presence/absence of *VRN-H2* (41%) and allelic variation at *Ppd-H1* (18%) and their interaction (16%; Supplemental Table S3). Consequently, overexpression of *HvFT3* controlled the expression of *VRN-H1* and *VRN-H2* and was therefore dominant over the repressive effects of the vernalization genes *VRN-H1* and *VRN-H2* on flowering.

We further investigated the effects of *HvFT3* on flowering time of winter barley in response to vernalization or SD treatment. For this purpose, we selected two groups of nontransgenic sister F_4 families from the cross *Ubi::HvFT3* × Igri to carry the photoperiod-responsive

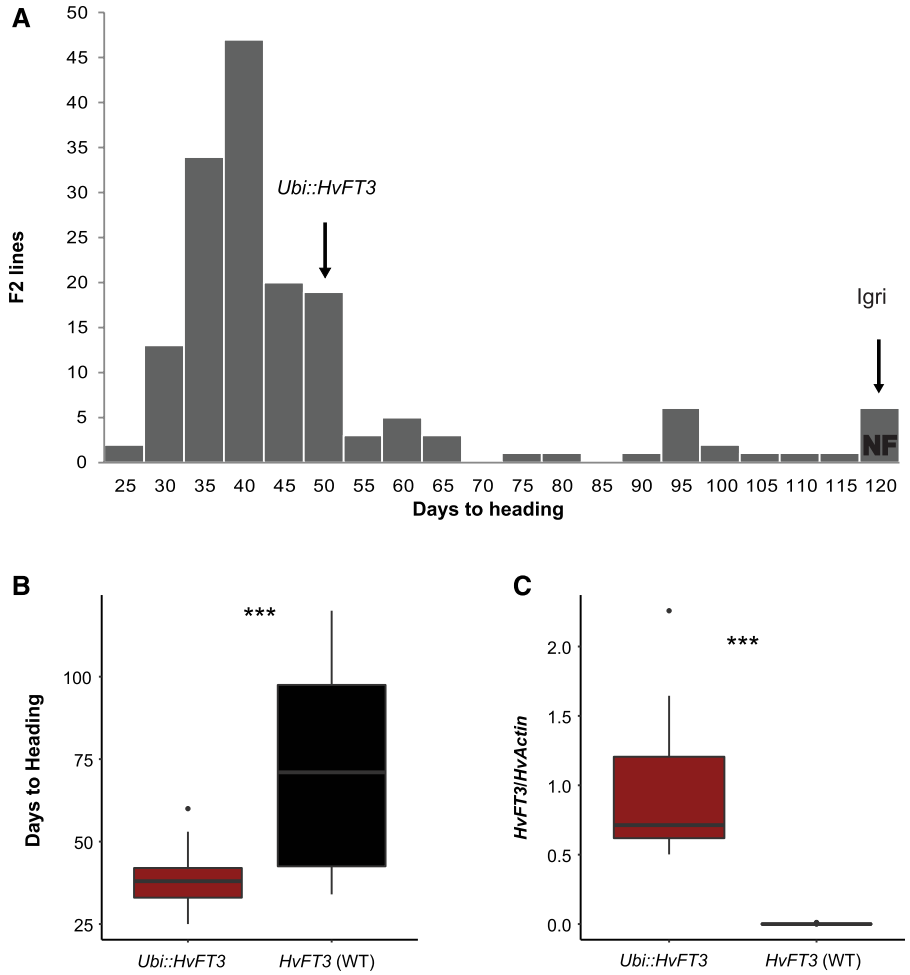

Figure 3. Flowering time and expression of *HvFT3* in the F_2 population *Ubi::HvFT3* × Igri grown under LD conditions. A, Distribution of flowering time in the *Ubi::HvFT3* × Igri F_2 lines. One hundred sixty-six F_2 plants derived from the cross *Ubi::HvFT3* × Igri were grown under LD conditions (16 h light). Plants were not subjected to vernalization, and flowering time was measured in days from germination until heading. The average flowering time of the two parental genotypes is indicated by arrows. NF, Did not flower after 120 d. B, Average flowering time and (C) expression of *HvFT3* normalized to *HvActin* of F_2 lines classified according to the presence/absence of the transgene *Ubi::HvFT3*. Expression analysis was performed on leaf samples from 69 selected F_2 lines collected 2 h before the end of the light period in LD (16 h light) at day 5 after germination. Error bars, standard deviation; WT, wild type. Significant differences were calculated based on a Student's *t* test. ***refers to a significant difference at $P < 0.001$.

allele *Ppd-H1*, the winter alleles *vrn-H1* and *VRN-H2*, and either the winter nonfunctional allele *hvft3* or the spring functional allele *HvFT3*. The two groups of genotypes were tested under two different treatments: vernalization for 8 weeks under LDs followed by LDs (VLD_LD) and 8 weeks under SDs followed by LDs (SD_LD; Fig. 5). In the VLD_LD treatment, *HvFT3* plants flowered at 31 DAG, which was significantly earlier than *hvft3* genotypes (42 DAG; Fig. 5). *HvFT3* plants in the SD_LD treatment required only 18 d to flower, while *hvft3* plants flowered 39 d after transfer to LDs. Consequently, natural variation at *HvFT3* affected flowering time under both conditions. The differences in flowering time between both groups of genotypes were, however, much more pronounced following the SD treatment compared to vernalization. We therefore concluded that *HvFT3* does not only counteract the repressive effect of the vernalization pathway but also induces early reproductive development of winter barley under SD conditions.

Transcriptional Changes at the SAM during the Vegetative and Early Reproductive Phases under LD and SD Conditions

Ubi::HvFT3 plants exhibited a faster initiation of spikelet primordia and an accelerated early reproductive development under LDs and SDs. We therefore aimed to detect candidate *HvFT3* targets that affected spikelet initiation and early reproductive development

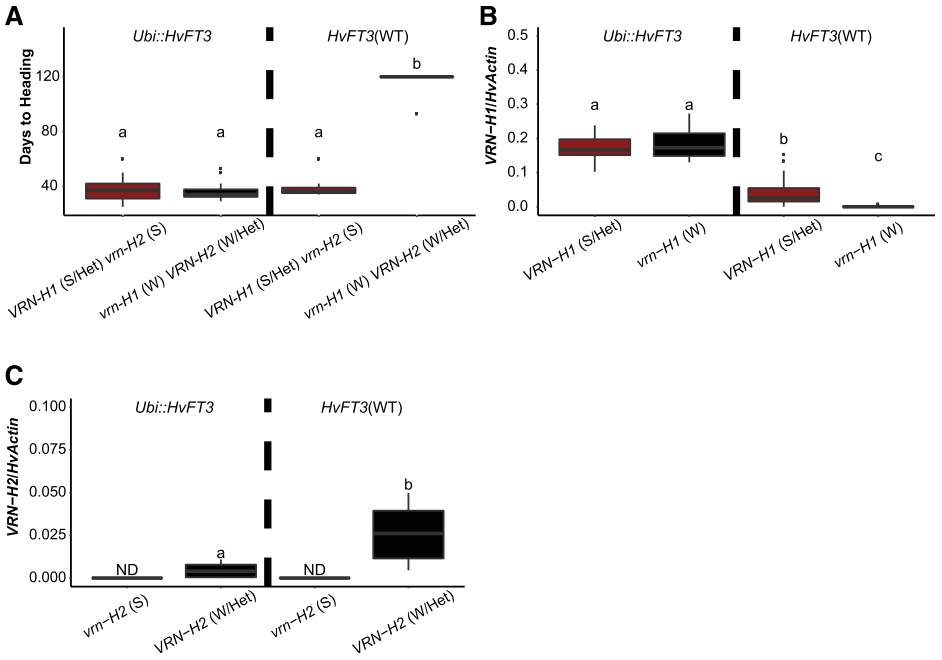

Figure 4. Effects of the transgene *Ubi::HvFT3* on flowering time, its interaction with allelic variation at *VRN-H1* and *VRN-H2*, and expression of *VRN-H1* and *VRN-H2* in the F_2 population *Ubi::HvFT3* × Igri under LD conditions. A, Average flowering time. B, Expression levels of *VRN-H1*. C, Expression levels of *VRN-H2*. F_2 lines were classified according to the presence of *Ubi*::*HvFT3* and allelic variation of *VRN-H1* and *VRN-H2*: S, Spring allele; Het, heterozygote; W, winter allele; WT, wild type. One hundred sixty-six F_2 lines derived from the cross *Ubi::HvFT3* × Igri were grown under LD conditions (16 h light). Plants were not subjected to vernalization, and flowering time was measured in days from germination until heading. Expression analysis was performed on leaf samples from 69 selected F_2 lines collected 2 h before the end of the light period in LD (16 h light) at day 5 after germination. Expression values were normalized to *HvActin*. Error bars, standard deviation. Significant differences were calculated based on a one-way ANOVA with a post-hoc Tukey HSD (honestly significant difference) test. Different letters above the columns indicate significant differences at $P < 0.05$. ND, Expression not detected.

independently of photoperiod. For this purpose, we conducted a global transcriptional profiling of MSA samples of *Ubi::HvFT3* and the null segregants collected at the spikelet initiation stage (W2.0) and at the stamen primordium stage (W3.0–3.5) under LD and SD conditions. We focused on transcripts that were differentially regulated between genotypes and stages under both photoperiods. Since a large number of transcripts have strong diurnal expression profiles that may vary between LDs and SDs, we did not compare transcript expression between photoperiods.

We detected a total of 20,282 transcripts with expression levels greater than five reads in at least three libraries under each condition (LD, SD). Differentially expressed transcripts (DETs) between genotypes and developmental stages were identified under both photoperiods. Principal component analysis demonstrated that the majority of transcripts were differentially regulated between stages, whereas DETs differentiated genotypes most strongly at the spikelet initiation stage (Supplemental Fig. S6). A total of 3,034 and 1,183 DETs were regulated between *Ubi::HvFT3* and the null segregant in at least one of the two stages under LDs and SDs, respectively. Between the stages, 4,824 transcripts were differentially regulated under LDs compared to 3,474 DETs under SDs in at least one of the genotypes (Fig. 6A). The detailed description of the expression of transcripts in the reference set in different genotypes, photoperiods, and developmental stages, and their functional annotations can be found in Supplemental Table S4.

At the spikelet initiation stage (W2.0), a total of 391 transcripts were differentially regulated between the transgenic plants and their null segregants under both photoperiods. Of these, 195 DETs were upregulated, 180 downregulated, and 16 differentially regulated under LDs and SDs in *Ubi::HvFT3* compared to the wild type (Fig. 6B). At the lemma primordium phase (W3.0–3.5), 154 transcripts were differentially regulated between genotypes under both photoperiods, with 84 DETs being upregulated and 69 downregulated and one transcript differentially regulated under LDs and SDs in *Ubi::HvFT3* compared to the null segregant (Supplemental Fig. S7). A subset of 92 transcripts were significantly affected by *Ubi::HvFT3* under both developmental stages and photoperiods. Consequently, overexpression of *HvFT3* affected more transcripts at the spikelet initiation than the lemma primordium stage under both photoperiods. In addition, the majority of transcripts regulated at the lemma primordium

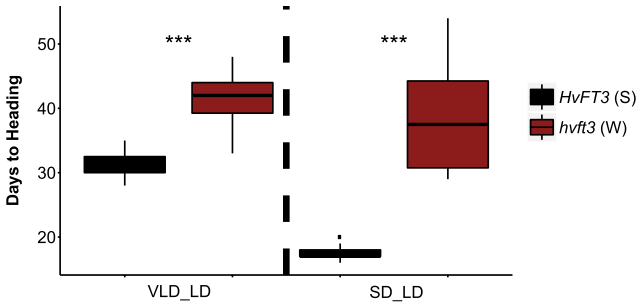

Figure 5. Effect of allelic variation at *HvFT3* on flowering time of winter barley grown under different experimental regimes. Flowering time of two winter F_4 families (*Ppd-H1 vrn-H1 VRN-H2*) carrying the spring (S) *HvFT3* (black) or the winter (nonfunctional, W) *hvft3* allele (red) was scored as days to heading after 8 weeks of vernalization in LD followed by LD (VLD_LD) and after 8 weeks of SD treatment followed by LD (SD_LD). Flowering time was measured in days from germination until heading. Each box represents the average flowering time of 10 plants. Error bars, standard deviation. Significant differences were calculated based on a Student's *t* test. ***refers to a significant difference in flowering time at $P < 0.001$.

stage were also differentially expressed between genotypes at the spikelet initiation stage.

Genes that were differentially regulated at the spikelet initiation stage had functions in meristem and floral development and hormone biosynthesis, signaling, and response. Among the transcripts strongly downregulated at the spikelet initiation stage in apices of the transgenic lines compared to the null segregants were transcription factors involved in the suppression of floral determinacy in Arabidopsis (Hartmann et al., 2000; Yant et al., 2010; Licausi et al., 2013; Huang et al., 2017). These included two homologs of MADS box transcription factors *AGAMOUS-LIKE1* (*HORVU6Hr1G002330*) and *SHORT VEGETATIVE PHASE* (*SVP*; *HORVU4Hr1G077850*), two *AP2*-like ethylene responsive-element-binding proteins (*AP2/EREB*; *HORVU7Hr1G116220*, *HORVU5Hr1G112440*) and AP2/B3 domain-containing proteins (*VRN1*; *HORVU5Hr1G017910*, *HORVU5Hr1G017890*; Fig. 7). In addition, in the transgenic line, we observed a reduced expression of an F-box-domain-containing protein *ABERRANT PANICLE ORGANIZATION1* (*HORVU7Hr1G108970*). In rice, an *ABERRANT PANICLE ORGANIZATION1* homolog suppresses the precocious conversion of inflorescence meristems to spikelet meristems (Ikeda et al., 2007).

Among the transcripts upregulated in the overexpression line were homologs of the *SQUAMOSA PROMOTER-BINDING-LIKE8* (*SPL8*; HORVU0Hr1G039150) and *SPL9* (*HORVU5Hr1G073440*) and a homolog of *LEAFY* (*LFY*; *HORVU2Hr1G102590*). We also observed higher expression levels for three cytochrome p450 monooxygenase proteins *CYP78A9* (*HORVU7Hr1G057100*), *CYP89A6* (*HORVU7Hr1G081610*), and *CYP71B34* (*HORVU7Hr1G096560*) in the transgenic compared to null segregants. Cytochrome P450 oxygenases and SPL proteins have been implicated in the control of leaf initiation, axillary meristem outgrowth, and floral development in model and crop plants (Miyoshi et al., 2004; Schwarz et al., 2008; Mascher et al., 2014; Gou et al., 2017). We also detected a strong up-regulation of homeobox-Leucine zipper protein family genes in the *Ubi::HvFT3* lines. These included *SIX-ROWED SPIKE1* (*VRS1*/*HvHOX1*; *HORVU2Hr1G092290*, *HORVU2Hr1G092300*), its close paralog, the homeobox gene *HOX2* (*HORVU2Hr1G036680*) and an additional homologous homeodomain zipper protein (*HORVU4Hr1G070610*). VRS1 has evolved specific functions to suppress the development of lateral spikelets and thus controls the dimorphism between two- and six-rowed barley spikes (Komatsuda et al., 2007). Interestingly, *VRS4* (*LATERAL ORGAN BOUNDARIES; LOB*; *HORVU3Hr1G016690*), the upstream positive regulator of *VRS1* (Koppolu et al., 2013) and another modifier of lateral spikelet development *INTERMEDIUM-C* (INT-C; *HORVU4Hr1G007040*; Ramsay et al., 2011) were also upregulated by *HvFT3* overexpression.

Transcripts related to hormone synthesis, signaling, and response were differentially regulated between genotypes. The transcript levels of a homolog of *GIBBERELLIN2-OXIDASE6* (*HORVU1Hr1G023460*) and a brassinosteroid responsive B-box zinc finger family protein *BZS1* (*HORVU7Hr1G091180*) were

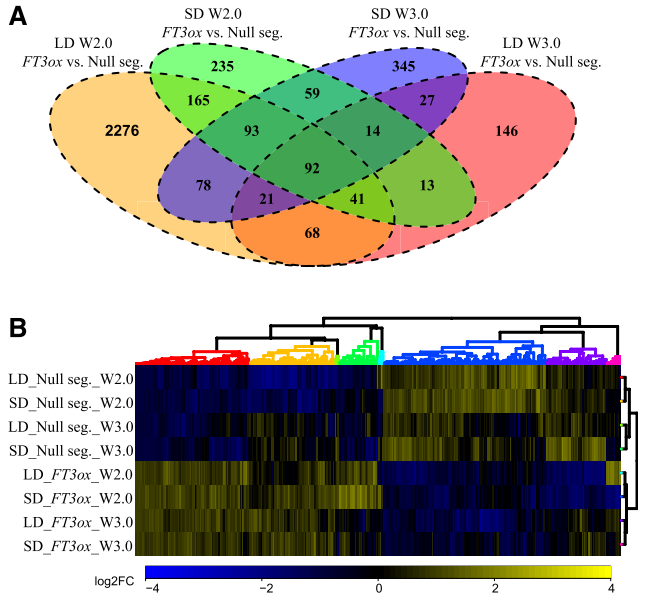

Figure 6. Global transcriptome analysis in developing main shoot apices in the *Ubi::HvFT3* and null segregant lines. A, Venn diagram of transcripts differentially regulated between *Ubi::HvFT3* (FT3ox) and the null segregant (Null seg.) at two different stages under LD and SD. B, Coexpression clustering of 391 DETs regulated between the *Ubi::HvFT3* and null segregant genotypes at the spikelet initiation stage. Colors represent log2 fold changes (log2-FC) in expression levels relative to the mean transcript abundance across the tested conditions. LD, Long day; SD, short day; W2.0, Waddington stage W2.0; W3.0, Waddington stage W3.0.

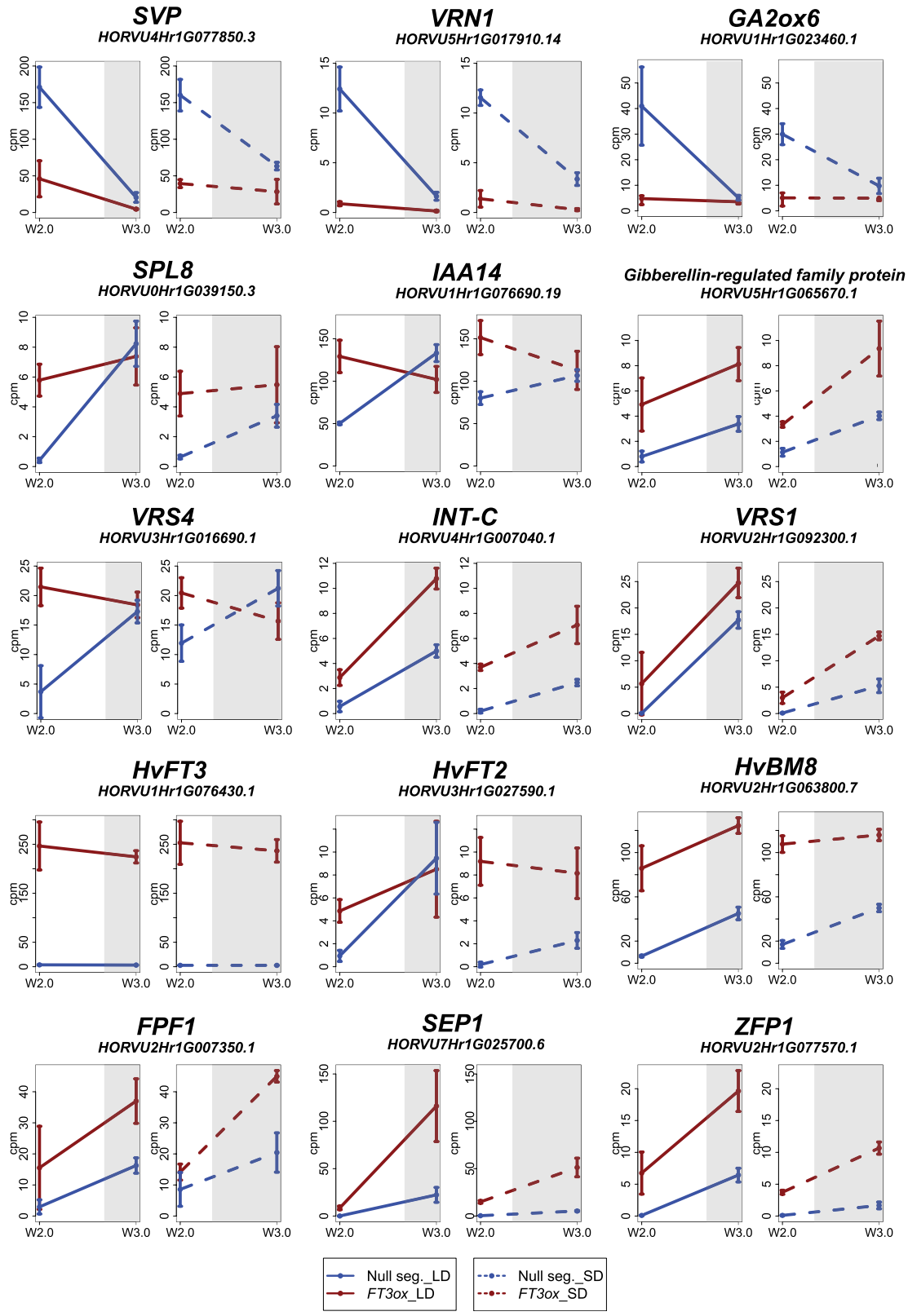

Figure 7. Expression profile of selected DETs. *Ubi::HvFT3* (red) and wild-type (blue) expression either at W2.0, W3.0, or both stages under long day (LD, left) and short day (SD, right) conditions. White, light period; gray, dark period. W, Waddington stage; cpm, counts per million.

reduced in the transgenic compared to wild-type lines. Several auxin-related genes, such as *INDOLEACETIC ACID-INDUCED PROTEIN14* (*IAA14*, *HORVU1Hr1G076690*), *IAA15* (*HORVU1Hr1G025670*), and *IAA17* (*HORVU3Hr1G031460*), a putative *INDOLE-3-ACETIC ACID-AMIDO SYNTHASE GH3.9* (*HORVU3Hr1G077360.1*), and an *AUXIN TRANSPORTER-LIKE1* (*HORVU3Hr1G084750*) were upregulated in the transgenic compared to the null segregant genotypes. These transcript changes suggested an increase in or redistribution of auxin and gibberellin concentration, which matched the earlier differentiation of spikelets and floral primordia in the transgenic line.

At the lemma primordium phase (W3.0–3.5), 154 transcripts were differentially regulated. Among those were genes implicated in meristem and floral development, disease resistance, and abiotic stress tolerance. Among the genes upregulated at both stages, W2.0 and W3.0, were the transgene *HvFT3* (*HORVU1Hr1G076430*) and its homolog *HvFT2* (*HORVU3Hr1G027590*), suggesting that *HvFT3* affects *HvFT2* expression in the MSA. We also detected the up-regulation of many floral homeotic genes that have conserved functions in controlling floral development across plant species. These included the *AP1*-like genes *HvBM3* (*HORVU0Hr1G003020*), *HvBM8* (*HORVU2Hr1G063800*), a Homeobox-Leu zipper protein homologous to *Arabidopsis thaliana HOMEOBOX* (*ATHB7*; *HORVU5Hr1G081090*), *SEPALLATA1* (*SEP1*; *HORVU7Hr1G025700*), and a *PISTILLATA* like gene (*PI*, *HORVU3Hr1G068900*). In addition, two SPL-like proteins, *SPL17* (*HORVU0Hr1G020810)* and *SPL16 (HORVU5Hr1G076380*), were expressed at higher levels in the transgenic than null segregant MSAs. SPLs are plant-specific transcription factors that play important roles in plant phase transition, the juvenile-to-adult vegetative transition, and the vegetative-to-reproductive transition and floral development (Hyun et al., 2017).

HvFT3 overexpression also caused an up-regulation of genes encoding proteins involved in light signaling such as *FAR-RED IMPAIRED RESPONSE1* homologs (*HORVU2Hr1G087170*, *HORVU3Hr1G011190*, *HORVU6Hr1G019030*) a homolog of *ELONGATED MESOCOTYL* (*HORVU5Hr1G059310*) essential for phytochrome synthesis, signaling, and light control of development in Arabidopsis (Sawers et al., 2004; Wang and Wang, 2015) and a basic helix-loop-helix protein (*HORVU0Hr1G017110*) involved in blue/far-red light signaling (Hyun and Lee, 2006; Castelain et al., 2012)

Furthermore, numerous genes regulated between genotypes were associated with the transport of carbon, nutrients, and ions including a *POLYOL/MONOSACCHARIDE TRANSPORTER1* (*HORVU2Hr1G036570*), metal ion transporters (*HORVU7Hr1G106570*, *HORVU1Hr1G071930*), amino acid transporters (*AMINO ACID PERMEASE*, *HORVU2Hr1G084780*; *BIDIRECTIONAL AMINO ACID TRANSPORTER1*, *HORVU3Hr1G053090*), and a sulfotransferase (*HORVU2Hr1G117700*). Furthermore, genes with functions in disease resistance were upregulated in the transgenic line, i.e. barley homologs of nucleotide-binding adaptor shared by APAF-1, R proteins, and CED-4 (NB-ARC) domain-containing disease resistance proteins (*HORVU3Hr1G002130*, *HORVU7Hr1G002260*, *HORVU7Hr1G002290*, *HORVU7Hr1G111700*).

Taken together, the overexpression of *HvFT3* altered the expression levels of genes involved in floral development, hormone homeostasis, and transport. Strong and precocious expression of genes with roles in floral development, spike architecture, and hormone homeostasis was linked to the earlier spikelet initiation observed in the *Ubi::HvFT3* plants.

DISCUSSION

HvFT3 Affects Spikelet Initiation But not Floral Development

HvFT3 (*Ppd-H2* locus) was originally described as a floral promoter under SD conditions in barley (Laurie et al., 1995; Laurie, 1997; Faure et al., 2007; Kikuchi et al., 2009). In this study, however, overexpression of *HvFT3* significantly accelerated flowering of spring barley under LDs but did not lead to successful flowering under SDs. In contrast to *HvFT3*, elevated expression levels of *HvFT1* were associated with day-neutral early flowering. For example, barley genotypes with a hypermorphic mutation in *PHYTOCHROME C*, a loss-of-function mutation in the circadian clock gene *EARLY FLOWERING3* and a hypomorphic mutation in the clock gene *LUX1/ARRHYTHMO* are characterized by photoperiod independent up-regulation of *HvFT1* and early flowering under long and short days (Faure et al., 2012; Campoli et al., 2013; Pankin et al., 2014). Consequently, *HvFT1* and *HvFT3* have different photoperiod-dependent effects on flowering; the induction of *HvFT1* but not *HvFT3* causes day length independent flowering in barley. Interestingly, overexpression of *HvFT3* in an Arabidopsis *ft* mutant resulted in a photoperiod-independent acceleration of flowering time. Both barley and Arabidopsis are considered long-day plants; however, both species differed in their response to photoperiod, and this difference was independent of *HvFT3* overexpression. It was previously shown that continuous exposure to long days is crucial for floral development and flowering in barley (Digel et al., 2015), whereas in Arabidopsis, a transient shift for a few days to LD growth conditions is sufficient to irreversibly commit the plants to flower (Corbesier et al., 2007).

Monitoring MSA development revealed that *HvFT3* overexpression specifically accelerated vegetative and early reproductive growth independently of photoperiod. Likewise, natural variation at *HvFT3* affected spikelet initiation and early reproductive growth under SDs and to a lesser extent under LDs. However, spring genotypes with the functional and nonfunctional

alleles of *HvFT3* failed to develop beyond the lemma primordium stage under SDs and inflorescences aborted. In contrast, variation in *HvFT1* expression levels as controlled by *Ppd-H1* were associated with the acceleration of all phases of MSA development under LDs, particularly the late reproductive phase of floral development (Hemming et al., 2008; Digel et al., 2015). Therefore, we propose that *HvFT3* specifically controls spikelet initiation but fails to promote floral development. Successful floral development likely depends on the LD induction of *HvFT1* expression.

In both Arabidopsis and temperate cereals, the vernalization and the photoperiod pathways converge on *FT* (Hemming et al., 2008; Amasino and Michaels, 2010). In barley, *VRN-H2* counteracts the LD activation of flowering by repressing *FT* expression before vernalization (Yan et al., 2006; Hemming et al., 2008; Mulki and von Korff, 2016). We showed that overexpression of *HvFT3* caused an up-regulation of the winter and spring alleles of *VRN-H1*, and this was associated with the down-regulation of *VRN-H2*. Consequently, transgenic winter lines flowered early without vernalization. Similarly, the functional *HvFT3* variant accelerated flowering time in winter genotypes grown under nonvernalizing conditions. Casao et al. (2011b) has already reported that *HvFT3* can significantly accelerate flowering of winter genotypes that were not or were only partially vernalized. In Arabidopsis, *FT* and *TWIN SISTER OF FT* suppress the late-flowering phenotype of winter accessions, even when *FLOWERING LOCUS C* was overexpressed (Michaels et al., 2005). Similarly, introducing the Hope-dominant allele of the wheat homolg *TaFT1*, which shows high transcript levels of *FT1*, into winter wheat led to an early-flowering phenotype (Yan et al., 2006). Consequently, *HvFT3* counteracts the repression of the vernalization pathway as demonstrated for the *FT1* homolog in wheat.

Interestingly, for plants with a functional *HvFT3* allele, treatment with SDs was significantly more effective than vernalization in promoting flowering. This indicated that *HvFT3* plays a major role in accelerating flowering of winter barley in response to SD treatment. Since *VRN-H2* is not expressed under SDs, *HvFT3* accelerates spikelet initiation of winter genotypes under SDs as already demonstrated for spring barley. Evans (1987) also found that development of the inflorescences in unvernalized winter wheat was more rapid under SDs than LDs. By showing that SDs actively induced development, our results thus supported the earlier proposed dual SD-LD induction of flowering in cereals (McKinney and Sando, 1935; Evans, 1987; Dubcovsky et al., 2006). *HvFT3* seems to play a dual role in the induction of flowering by promoting spikelet initiation under SDs and by reducing the requirement for vernalization under LDs as HvFT3 caused a down-regulation of *VRN-H2* in the absence of vernalization.

High levels of *VRN-H1* caused an up-regulation of *HvFT1* (Hemming et al., 2008), and a positive feedback loop between *VRN1* and *FT* has been suggested in wheat (Shimada et al., 2009; Distelfeld and Dubcovsky, 2010). Furthermore, Deng et al. (2015) have suggested that *VRN-H1* upregulates *HvFT1* by directly binding to its promoter. In this study, however, the strong and early up-regulation of *VRN-H1* in *Ubi::HvFT3* plants under LDs and SDs was not associated with a consistent up-regulation of *HvFT1*. This is in contrast to results from Casao et al. (2011a), who demonstrated that the up-regulation of the native *HvFT3* transcript correlated with increased levels of *VRN-H1* and *HvFT1* expression. However, in the transgenic lines, relatively high expression levels of *VRN-H1* were not correlated with an induction of *HvFT1* expression levels as normally observed in wild-type plants. This altered ratio of high-*VRN-H1* and low-*HvFT1* expression in the transgenic lines may explain the observed early abortion of the main inflorescence of some transgenic plants (Supplemental Fig. S3). While overexpression of *HvFT3* did not clearly affect *HvFT1* expression levels, we demonstrated that native *HvFT3* expression levels were influenced by natural variation at *Ppd-H1* and thus differences in *HvFT1* expression levels. This is in contrast to results in a transgenic wheat line carrying a highly expressed *FT1* allele, where *FT3* expression levels were increased under both LDs and SDs, while in wheat and Brachypodium (*Brachypodium distachyon* L.) $FT1_{RNAi}$ lines, *FT3* expression levels were not altered (Lv et al., 2014). Similarly, in rice, cosilencing of the *FT1* homologs *HEADING DATE3a* and *RFT1* also showed no effect on the expression of the rice homologs of *FT3* (Komiya et al., 2008). However, expression profiling of FT-like genes in the cultivar Morex demonstrated that *HvFT3* expression preceded the expression of *HvFT1*, but *HvFT3* expression levels decreased when *HvFT1* expression increased (Kikuchi et al., 2009). These findings support our results that in barley *HvFT1* expression is associated with a down-regulation of *HvFT3* transcript levels.

Overexpression of *HvFT3* Induces the Expression of Floral Regulators and Row-Type Genes

We used whole-transcriptome sequencing in the dissected MSAs at the spikelet initiation and lemma primordium stages to identify *HvFT3*-dependent molecular changes observed under both photoperiods. Early spikelet initiation in the transgenic lines was associated with a down-regulation of putative floral repressors in the MSA. These included an *SVP*-like gene, which delays floral transition by repressing the flowering pathway integrators *FT*, *FLOWERING LOCUS D*, the MADS domain gene *SUPPRESSOR OF OVEREXPRESSION OF CONSTANS1* (*SOC1*) and gibberellin biosynthesis in Arabidopsis (Lee et al., 2007; Li et al., 2008; Andrés et al., 2014). We also observed an *HvFT3*-dependent down-regulation of floral homeotic genes with an *AP2* domain, i.e. *VRN1* (*AP2/B3*) and *AP2/EREB*. *AP2* transcription factors play essential roles in growth, development, and stress response and have been implicated in various signal transduction pathways mediated by hormones such as abscisic acid,

ethylene, cytokinin, and jasmonate (Yant et al., 2010). The transcription of floral activators like *SOC1* and *FT* is directly repressed by proteins with an *AP2* domain and a B3-type DNA binding domain (Castillejo and Pelaz, 2008; Yant et al., 2010) and overexpression of AP2 domain-containing proteins causes late flowering in Arabidopsis (Aukerman and Sakai, 2003; Schmid et al., 2003; Chen, 2004; Jung et al., 2007). The down-regulation of *AP2/EREB* (*AP2*) and *VRN1* (*AP2/B3*) has previously been associated with spikelet initiation in barley (Digel et al., 2015). Thus, their down-regulation by *HvFT3* overexpression might have accelerated the transition to reproductive growth in the transgenic lines.

The strong down-regulation of a *GIBBERELLIN2-OXIDASE6* that initiates the major catabolic pathway for gibberellin (GA) suggested that spikelet initiation co-occurred with an increase in GA in the shoot apex. Pearce et al. (2013) have shown that the induction of *FT1* expression causes the up-regulation of GA biosynthetic genes in the shoot apex. The authors proposed that *FT1* is expressed in the leaves and the protein is then transported to the SAM, where it induces GA biosynthetic genes necessary for the up-regulation of the early floral meristem genes and development of the wheat spike. Similarly in rice, *GA2ox1* expression is strongly decreased in the shoot apex at the transition from vegetative to reproductive growth, and ectopic expression of *OsGA2OX1* in transgenic rice inhibits stem elongation and the development of reproductive organs (Sakamoto et al., 2001). Our expression analysis suggested that the up-regulation of *FT3* also causes GA levels to rise in the MSA, as has been shown for *FT1* in wheat. The up-regulation of several auxin-related genes, such as indole-3-acetic acid-like and auxin transporter genes, suggested that *HvFT3* overexpression also induced changes in auxin homeostasis at the MSA. An increase in auxin may be important for floral organ initiation in barley, as demonstrated in Arabidopsis, where auxin distribution within the periphery of the inflorescence meristems specifies the site of floral meristem initiation and mediates organ growth and patterning (Krizek, 2011).

Down-regulation of putative floral repressors was correlated with an up-regulation of *SPL8* and *SPL9* specifically at spikelet initiation. The up-regulation of *SPL* genes in the transgenic plants was associated with an up-regulation of genes putatively involved in floral development such as *LFY*, *AP1*, and *FUL*-like genes at spikelet initiation and the lemma primordium stage. In Arabidopsis, *SPL* genes are repressed by *SVP* (Torti et al., 2012), and SPL proteins control floral transition by binding directly to and activating the transcription of *SOC1*, *AP1*, *FUL*, and *LFY* (Wang et al., 2009; Yamaguchi et al., 2009). These results suggested that *HvFT3* regulates floral integrator genes as shown for *HvFT1* (Digel et al., 2015) and that gene regulatory networks controlling floral transition are at least in part conserved between Arabidopsis and barley.

At the lemma primordium stage, overexpression of *HvFT3* induced the expression of barley homologs of the Arabidopsis floral homeotic genes *AP1/FUL*, *SEP1*, *SEP3*, and *PI*, which are involved in floral organ formation (Mandel et al., 1992; Goto and Meyerowitz, 1994; Pelaz et al., 2000). These transcripts were upregulated under LD and SD conditions, even though successful floral development only proceeded under LDs. Interestingly, *HvFT3* overexpression also induced the expression of the row-type genes *VRS1*, *VRS4*, and *INT-C*. *VRS4* encodes a *LATERAL ORGAN BOUNDARY* transcription factor that is homologous to maize *RAMOSA2* and upregulates the expression of the a HD-ZIP transcription factor *VRS1* (*HvHox1*; Koppolu et al., 2013). *VRS1* is a key inhibitor of lateral spikelet development, and loss of function or a complete down-regulation leads to the development of six-rowed spikes. A partial down-regulation of *VRS1* as observed in *intermedium* (*int*) mutants results in an *intermedium spike* phenotype with varying two- or six-rowed patterns or enlarged lateral florets, which may or may not develop into kernels depending on the position on the spike and the environment. The most frequent *int* mutant is *int-c*, which has been identified as a barley homolog of *TEOSINTE-BRANCHED1*, a TCP transcription factor and major domestication-related gene affecting shoot branching in maize. Boden et al. (2015) have shown that a modified spikelet arrangement in wheat is controlled by FT1, where higher levels of *FT1* expression as controlled by *PPD1* inhibited paired spikelet formation. We show that modulated expression of an *FT*-like gene in barley acts upstream of important row-type genes and thus provides a direct link between a flowering gene and spike architecture.

CONCLUSION

Overexpression of *HvFT3* accelerated the spikelet initiation and the early reproductive development of spring barley independently of the photoperiod but did not accelerate floral development. Transgenic lines did not flower under SD conditions, suggesting that overexpression of *HvFT3* could not compensate for an LD-dependent signal necessary for successful floral development. This strongly suggests that *HvFT3* is functionally different from *HvFT1*, which has been associated with both spikelet initiation and floral development. *HvFT3* was dominant over the repressive effect of the vernalization pathway and induced spikelet initiation of winter and spring barley under SD conditions. *HvFT3* overexpression modified the expression of a number of floral regulators, floral homeotic genes, and genes involved in GA and auxin synthesis, signaling, and response pathways in the shoot apex. It also upregulated the expression of barley row-type genes *VRS4*, *VRS1*, and *INT-C*, which suggested that *FT*-like genes may control spike architecture in addition to modulating developmental timing.

MATERIALS AND METHODS

Generation and Growth Conditions of Transgenic *Ubi::HvFT3* Lines

Barley (*Hordeum vulgare*) plants of the spring variety Golden Promise were transformed with an overexpression construct generated with the genomic DNA clones of *HvFT3* from Golden Promise driven by the maize (*Zea mays*) ubiquitin promoter (Ubi-I; Christensen et al., 1992). The overexpression cassette was inserted into the pWBVEC8 binary vector (Wang et al., 1998) and introduced into *Agrobacterium tumefaciens*. *A. tumefaciens*-mediated transformation was then performed on excised barley embryos (Tingay et al., 1997; Matthews et al., 2001).

Independent barley transformants were regenerated, and T_1 and T_2 plants were screened for the presence of the transgene using two pairs of primers that bind to the hygromycin selectable marker gene and the *HvFT3* genomic DNA (gDNA) sequence (Supplemental Table S5).

Five independent transgenic T_2 families designated as *Ubi::HvFT3* lines N1, N2, N4, N16, and N23, in addition to two control lines, a null segregant line that does not carry the transgene, and Golden Promise, were all sown in soil and grown under SDs (8 h light/16 h dark) and LDs (16 h light/8 h dark) in the greenhouse (temperature 20°C/16°C days/nights). Four to 15 plants of each of the lines were used to score flowering time, which was measured in days from germination until heading (days after germination [DAG]). Heading was scored as the emergence of spike awns out of the sheath of the main shoot flag leaf (Zadoks stage 49; Zadoks et al., 1974), and the experiment was stopped 120 DAG under SDs. For each tested line, leaf material from every plant (each plant represents a biological replicate) was collected 5 DAG, 2 h before the end of the light (Zeitgeber, T14 in LD and T6 in SD) to perform RNA extraction and gene expression analysis. In addition, expression of *HvFT3* and *HvFT1* was surveyed in transgenic, null, and wild-type genotypes during development and 6, 13, 20, and 28 d after sowing under LD conditions. Leaf samples were harvested 2 h before the end of the day, and three biological replicates were analyzed per line and time point.

We further examined whether variation at *Ppd-H1* affected *HvFT3* expression in wild-type plants under LDs and SDs. For this purpose, we evaluated *HvFT3* expression levels in Golden Promise (*ppd-H1*) and a derived introgression line with a wild-type *Ppd-H1* allele from the winter barley Igri over development under LDs and SDs. Three replicate leaves per genotype and time point were harvested 2 h before the end of the day for RNA extraction and expression analysis.

Generation of Arabidopsis Transgenic *35S::HvFT3* Lines and Their Growth Conditions

The genomic DNA of *HvFT3* from Golden Promise was ligated into a 35S promoter-driven pLeela binary vector following the manufacturer's instructions (Invitrogen). The resulting construct was introduced into the Arabidopsis (*Arabidopsis thaliana*) *ft-10* mutant (Transfer DNA, T-DNA insertion alleles in the Columbia background; Yoo et al., 2005) through *A. tumefaciens*-mediated transformation by the floral-dip method (Clough and Bent, 1998). An empty pLeela vector was also introduced into *ft-10* to serve as a control line (mock). *35S::FT* seeds were kindly provided by Dr. Fernando Andres. Plants from three independent *ft-10 35S::HvFT3* lines in addition to the mock, *35S::FT*, and *ft-10* lines were grown in the greenhouse under LD (16 h light/8 h dark) and SD (8 h light/16 h dark) at a temperature of 21°C/19°C light/dark. Flowering-time was measured as the total number of leaves when the first flower opened. Seven to 12 plants per line were scored.

Inflorescence Development of Transgenic *Ubi::HvFT3* Lines

Transgenic *Ubi::HvFT3* plants in addition to null segregant and wild-type Golden Promise plants were grown under SDs (8 h light/16 h dark) or LDs (16 h light/8 h dark) in the greenhouse (temperature 20°C/16°C days/nights). The transgenic T_4 plants grown under SD and LD were generated from lines N23 and N16, respectively. Primary shoots of *Ubi::HvFT3*, null segregant, and wild-type plants were dissected each 2 to 3 d under LD and 6 to 8 d under SD. Two to four replicates were dissected at each time point. Phenotypic changes of the SAM were monitored and evaluated according to the Waddington scale for inflorescence development (Waddington et al., 1983).

Generation and Growth Conditions of *Ubi::HvFT3* × Igri F_2 Population

The transgenic line *Ubi::HvFT3* N23 was crossed with the winter barley variety Igri. Golden Promise (wild type), the genetic background of the transgenic line, is a spring variety that carries a functional allele of the *HvFT3* gene (Laurie et al., 1995; Faure et al., 2007). Golden Promise also carries a mutation in the *CONSTANS*, *CONSTANS*-like and *TOC1* (CCT) domain of *Ppd-H1*, which causes reduced photoperiod sensitivity and delayed flowering under LDs (Turner et al., 2005). In addition, Golden Promise is characterized by a spring allele at *VRN-H1* and a deletion of the *VRN-H2* locus and consequently does not require vernalization for the induction of flowering. In contrast, Igri carries the winter null allele of *HvFT3*, a dominant *Ppd-H1* allele with a strong photoperiod response, and winter alleles at *VRN-H1* and *VRN-H2* and thus needs vernalization to flower.

One hundred and sixty-six F_2 plants derived from the cross *Ubi::HvFT3* × Igri were sown in soil and grown in the greenhouse (temperature 20°C/16°C days/nights) under LD (16 h/8 h light/dark) conditions. Seedlings were not subjected to vernalization, and flowering time was scored as number of days until heading (Zadoks stage 49). Leaf material was harvested from parental lines and 69 F_2 lines 5 DAG at T14 under LD and subsequently used for RNA extraction and gene expression analysis. The selection of F_2 lines for gene expression analysis under LD was based on the genotypic information to ensure balanced allele combinations at the analyzed flowering time genes (the transgene, *HvFT3* [wild type], *Ppd-H1*, *VRN-H1*, and *VRN-H2*).

Generation and Growth Conditions of *HvFT3* F_4 Spring Families

For testing the effect of natural variation at *HvFT3* on MSA development, three F_2:F_4 families were selected from the cross *Ubi::HvFT3* × Igri that varied at *HvFT3* but carried spring alleles at *Ppd-H1*, *VRN-H1*, and *VRN-H2*. The development of the MSA of these selected families was scored under SD (8 h light/16 h dark, temperature 20°C/16°C) and LD (13 h light/11 h dark, temperature 20°C/16°C). Primary shoots of six plants from each allelic combination (two plants/family) were dissected each 3 to 7 and 6 to 10 d, under LDs and SDs, respectively. None of the plants reached heading under SDs, whereas only some plants did not flower by 120 DAG and were given a score of 120 DAG.

Generation, Growth Conditions, and the Vernalization/SD Response Experiment of *HvFT3* F_4 Winter Families

Four nontransgenic F_2:F_4 families were developed from selected F_2 lines of the cross *Ubi::HvFT3* × Igri. Plants of the developed families carried the winter alleles *vrn-H1* and *VRN-H2*, the photoperiod-responsive allele *Ppd-H1*, and either the winter null allele *hvft3* or the spring functional allele *HvFT3*. Plants from both families were grown under two different treatments: VLD_LD, 8 weeks of vernalization under LDs (16 h light/8 h dark, temperature 4°C) followed by LDs (16 h light/8 h dark, temperature 20°C/16°C); and SD_LD, 8 weeks of SDs (8 h light/16 h dark, temperature 20°C/16°C) followed by LDs (16 h light/8 h dark, temperature 20°C/16°C). Flowering time was scored for 10 plants per treatment and genotype.

DNA Extraction and Genotyping of the Segregating Populations

Genomic DNA of individual F_2 genotypes was extracted from leaf samples following the Biosprint DNA extraction protocol (Qiagen). F_2 genotypes of all analyzed populations were genotyped for the presence of the transgene and allelic diversity of the major flowering genes *Ppd-H1* (Turner et al., 2005), *VRN-H1* (Hemming et al., 2009), *VRN-H2* (Dubcovsky et al., 2005), and *HvFT3* (Faure et al., 2007; Kikuchi et al., 2009). Polymerase chain reactions (PCRs) were performed as described in the original references (list of primers in Supplemental Table S5).

RNA Extraction, cDNA Synthesis, and Reverse Transcription Quantitative PCR

Total RNA extraction, first-strand cDNA synthesis, and reverse transcription quantitative PCR (RT-qPCR) for transgenic and wild-type plants as well as F_2 plants were performed as described in Campoli et al. (2012). RT-qPCR was performed using gene-specific primers (Supplemental Table S5). Two technical replicates were used for each cDNA sample, and starting amounts for each data point were calculated based on the titration curve for each target gene and the reference (*HvActin*) gene using the LightCycler 480 Software (Roche; version 1.5).

Statistical Analysis

The statistical significance of differences in flowering time and gene expression levels between each of the *Ubi::HvFT3* genotypes and the wild-type and the null controls (wild type + Null combined) grown under LDs and SDs was determined using Student's *t* test. A fixed-model ANOVA for unbalanced designs was used to calculate significant effects and two-way interaction effects of the transgene and allelic variation at *Ppd-H1*, *VRN-H1*, *VRN-H2*, and *HvFT3* on flowering time and gene expression in all tested F2 populations. Pearson correlation coefficients were calculated between flowering time and gene expression values in the tested population.

RNA Sequencing Experiment and Analysis

RNA was isolated from tissue of the MSA harvested from *Ubi::HvFT3* and null segregant plants grown under LD and SD conditions. MSA tissue was harvested at the developmental stages W2.0 and W3.0 to 3.5 2 h before the end of the light period. Leaves surrounding the MSA were removed manually, and the apex was cut using a microsurgical stab knife (5-mm blade at 15° [SSC#72-1551]). For each of three biological replicates, at least 10 MSA were pooled. The MSA harvested for RNA extraction were frozen immediately in liquid nitrogen and stored at −80°C. The RNA was isolated as described in van Esse et al. (2017). The Illumina cDNA libraries were prepared according to the TruSeq RNA sample preparation (version 2; Illumina). A cBot (Illumina) was used for clonal sequence amplification and generation of sequence clusters. Single-end sequencing was performed using a HiSeq 2500 (Illumina) platform by multiplexing 8 libraries resulting in ∼18 million reads per library. The sequencing data quality was verified using FastQC software (version 0.10.1, http://www.bioinformatics.bbsrc.ac.uk/projects/fastqc/) before further processing using the CLC Genomics workbench (version 6.0.4, CLCbio). PCR duplicates were removed from the raw sequencing data using the Duplicate Read Removal plugin of CLC. The reads were trimmed with an error probability limit calculated from the Phred scores of 0.05, allowing for a maximum of two ambiguously called nucleotides per read. Reads shorter than 60 bp, subsequent to the quality-based trimming, were removed from the dataset.

The obtained RNA sequencing reads were mapped to a barley high confidence transcripts reference (Beier et al., 2017; Mascher et al., 2017) using Salmon in quasi-mapping-based mode as described in van Esse et al. (2017). When building the quasi-mapping-based index, an auxiliary k-mer hash over k-mers of length 31 was used. U (unstranded single end read) was chosen as library type to quantify the reads of each library. The expected number of reads (NumReads) that have originated from each transcript given the structure of the uniquely mapping and multimapping reads and the relative abundance estimates for each transcript and transcripts per million values were extracted using Salmon (Patro et al., 2017). The NumReads was used in downstream analysis. Transcripts with expression levels greater than five NumReads in at least three libraries under each condition (LD, SD) were retained. The expected number of reads and normalized counts per million values are provided in Supplemental Table S4. Differentially regulated reads were called using the R bioconductor package Limma-vroom (Ritchie et al., 2015) using a Benjamin and Hochberg adjustment for multiple testing for calculation of the adjusted *P* values (false discovery rate; FDR values). For expression analysis, an FDR value of 0.05 was used as cut-off value for the selection of differentially-expressed transcripts (DETs). DETs were extracted per developmental stage between the genotypes and per genotype between the developmental stages. Hierachical cluster analysis was done in R using Pearson correlation coefficients. The overrepresentation analysis of particular GO terms was performed using the R-package TopGo (Alexa and Rahnenfuhrer, 2016). The Venn diagram was drawn using the R package VennDiagram (Chen and Boutros, 2011). The correspondence of MLOC to HORVU gene identifiers was estimated using reciprocal blastn analysis (identity score > 95%). The gene names were extracted based on the MLOC identifiers as annotated in Digel et al. (2015).

Illumina data is available in the European Short Read Archive, EBI ArrayExpress E-MTAB-7158. Accession numbers of major flowering-time genes are listed in Supplemental Table S5.

Supplemental Data

The following supplemental materials are available.

Supplemental Figure S1. Expression of *HvFT3* and *HvFT1* in *Ubi::HvFT3* transgenic lines, null segregant and Golden Promise plants 6, 13, 20, and 28 d after germination under LD conditions.

Supplemental Figure S2. Expression of *HvFT3* in Golden Promise (GP) and a derived introgression line with a wild-type *Ppd-H1* allele under LDs and SDs at 6, 13, 20, and 28 d after germination.

Supplemental Figure S3. Developing shoot apices in wild-type and transgenic plants.

Supplemental Figure S4. Complementation experiment in Arabidopsis.

Supplemental Figure S5. Effects of the transgene *Ubi::HvFT3* and its interaction with allelic variation at *Ppd-H1* on flowering time of the F_2 population *Ubi::HvFT3* × Igri under LD conditions.

Supplemental Figure S6. Principal component analysis of normalized expression from all expressed genes under LDs and SDs.

Supplemental Figure S7. Coexpression clustering of 154 DETs regulated between the *Ubi::HvFT3* and null segregant genotypes at the lemma primordium stage.

Supplemental Table S1. ANOVA of flowering time of the F_2 population *Ubi::HvFT3* × Igri grown under LD conditions.

Supplemental Table S2. Pearson correlation coefficients of flowering time and expression levels of tested flowering genes in the F_2 population *Ubi::HvCFT3* × Igri grown under LD conditions.

Supplemental Table S3. ANOVA of expression of all tested flowering genes in the F_2 population *Ubi::HvFT3* × Igri grown under LD conditions.

Supplemental Table S4. Annotation of differentially expressed transcripts, log-fold change, FDR values, number of reads, and normalized counts per million values per genotype, photoperiod, stage, and replicate.

Supplemental Table S5. List of primers used in this study.

ACKNOWLEDGMENTS

The authors cordially thank Kerstin Luxa, Caren Dawidson, and Andrea Lossow for excellent technical assistance and Chiara Campoli for preparing the *Ubi::HvFT3* constructs.

Received February 23, 2018; accepted August 30, 2018; published September 13, 2018.

LITERATURE CITED

Abe M, Kobayashi Y, Yamamoto S, Daimon Y, Yamaguchi A, Ikeda Y, Ichinoki H, Notaguchi M, Goto K, Araki T (2005) FD, a bZIP protein mediating signals from the floral pathway integrator FT at the shoot apex. Science **309**: 1052–1056

Alexa A, Rahnenfuhrer J (2016) topGO: Enrichment Analysis for Gene Ontology. R package version 2.30.0.

Amasino RM, Michaels SD (2010) The timing of flowering. Plant Physiol **154**: 516–520

Andrés F, Coupland G (2012) The genetic basis of flowering responses to seasonal cues. Nat Rev Genet **13**: 627–639

Andrés F, Porri A, Torti S, Mateos J, Romera-Branchat M, García-Martínez JL, Fornara F, Gregis V, Kater MM, Coupland G (2014) SHORT VEGETATIVE PHASE reduces gibberellin biosynthesis at the Arabidopsis shoot

apex to regulate the floral transition. Proc Natl Acad Sci USA **111**: E2760–E2769

Appleyard M, Kirby EJM, Fellowes G (1982) Relationships between duration of phases in the pre-anthesis life cycle of spring barley. Aust J Agric Res **33**: 917–925

Araki T (2001) Transition from vegetative to reproductive phase. Curr Opin Plant Biol **4**: 63–68

Aukerman MJ, Sakai H (2003) Regulation of flowering time and floral organ identity by a MicroRNA and its APETALA2-like target genes. Plant Cell **15**: 2730–2741

Ballerini ES, Kramer EM (2011) In the light of evolution: a reevaluation of conservation in the CO-FT regulon and its role in photoperiodic regulation of flowering time. Front Plant Sci **2**: 81

Beier S, Himmelbach A, Colmsee C, Zhang XQ, Barrero RA, Zhang Q, Li L, Bayer M, Bolser D, Taudien S, (2017) Construction of a map-based reference genome sequence for barley, *Hordeum vulgare* L. Sci Data **4**: 170044

Boden SA, Cavanagh C, Cullis BR, Ramm K, Greenwood J, Jean Finnegan E, Trevaskis B, Swain SM (2015) Ppd-1 is a key regulator of inflorescence architecture and paired spikelet development in wheat. Nat Plants **1**: 14016

Boss PK, Bastow RM, Mylne JS, Dean C (2004) Multiple pathways in the decision to flower: enabling, promoting, and resetting. Plant Cell 16 (Suppl): S18–S31

Campoli C, von Korff M (2014) Genetic Control of Reproductive Development in Temperate Cereals. *In* **J-P Jacquot, P Gadal, F Fornara**, eds, Advances in Botanical Research: Vol. 72. The Molecular Genetics of Floral Transition and Flower Development. Academic Press, San Diego, CA, pp 131–158.

Campoli C, Drosse B, Searle I, Coupland G, von Korff M (2012) Functional characterisation of HvCO1, the barley (*Hordeum vulgare*) flowering time ortholog of CONSTANS. Plant J **69**: 868–880

Campoli C, Pankin A, Drosse B, Casao CM, Davis SJ, von Korff M (2013) HvLUX1 is a candidate gene underlying the early maturity 10 locus in barley: phylogeny, diversity, and interactions with the circadian clock and photoperiodic pathways. New Phytol **199**: 1045–1059

Casao MC, Igartua E, Karsai I, Lasa JM, Gracia MP, Casas AM (2011a) Expression analysis of vernalization and day-length response genes in barley (*Hordeum vulgare* L.) indicates that VRNH2 is a repressor of PPDH2 (HvFT3) under long days. J Exp Bot **62**: 1939–1949

Casao MC, Karsai I, Igartua E, Gracia MP, Veisz O, Casas AM (2011b) Adaptation of barley to mild winters: a role for PPDH2. BMC Plant Biol **11**: 164

Castelain M, Le Hir R, Bellini C (2012) The non-DNA-binding bHLH transcription factor PRE3/bHLH135/ATBS1/TMO7 is involved in the regulation of light signaling pathway in Arabidopsis. Physiol Plant **145**: 450–460

Castillejo C, Pelaz S (2008) The balance between CONSTANS and TEMPRANILLO activities determines FT expression to trigger flowering. Curr Biol **18**: 1338–1343

Chardon F, Damerval C (2005) Phylogenomic analysis of the PEBP gene family in cereals. J Mol Evol **61**: 579–590

Chen X (2004) A microRNA as a translational repressor of APETALA2 in Arabidopsis flower development. Science **303**: 2022–2025

Chen H, Boutros PC (2011) VennDiagram: a package for the generation of highly-customizable Venn and Euler diagrams in R. BMC Bioinformatics **12**: 35

Christensen AH, Sharrock RA, Quail PH (1992) Maize polyubiquitin genes: structure, thermal perturbation of expression and transcript splicing, and promoter activity following transfer to protoplasts by electroporation. Plant Mol Biol **18**: 675–689

Clough SJ, Bent AF (1998) Floral dip: a simplified method for Agrobacterium-mediated transformation of Arabidopsis thaliana. Plant J **16**: 735–743

Corbesier L, Vincent C, Jang S, Fornara F, Fan Q, Searle I, Giakountis A, Farrona S, Gissot L, Turnbull C, (2007) FT protein movement contributes to long-distance signaling in floral induction of Arabidopsis. Science **316**: 1030–1033

Danilevskaya ON, Meng X, Hou Z, Ananiev EV, Simmons CR (2008) A genomic and expression compendium of the expanded PEBP gene family from maize. Plant Physiol **146**: 250–264

Deng W, Casao MC, Wang P, Sato K, Hayes PM, Finnegan EJ, Trevaskis B (2015) Direct links between the vernalization response and other key traits of cereal crops. Nat Commun6: 5882

Digel B, Pankin A, von Korff M (2015) Global transcriptome profiling of developing leaf and shoot apices reveals distinct genetic and environmental control of floral transition and inflorescence development in barley. Plant Cell **27**: 2318–2334

Digel B, Tavakol E, Verderio G, Tondelli A, Xu X, Cattivelli L, Rossini L, von Korff M (2016) Photoperiod-H1 (Ppd-H1) controls leaf size. Plant Physiol **172**: 405–415

Distelfeld A, Dubcovsky J (2010) Characterization of the maintained vegetative phase deletions from diploid wheat and their effect on VRN2 and FT transcript levels. Mol Genet Genomics **283**: 223–232

Dubcovsky J, Chen C, Yan L (2005) Molecular characterization of the allelic variation at the VRN-H2 vernalization locus in barley. Mol Breed **15**: 395–407

Dubcovsky J, Loukoianov A, Fu D, Valarik M, Sanchez A, Yan L (2006) Effect of photoperiod on the regulation of wheat vernalization genes VRN1 and VRN2. Plant Mol Biol **60**: 469–480

Ejaz M, von Korff M (2017) The genetic control of reproductive development under high ambient temperature. Plant Physiol **173**: 294–306

Evans LT (1987) Short day induction of inflorescence initiation in some winter wheat varieties. Aust J Plant Physiol **14**: 277–286

Faure S, Higgins J, Turner A, Laurie DA (2007) The FLOWERING LOCUS T-like gene family in barley (Hordeum vulgare). Genetics **176**: 599–609

Faure S, Turner AS, Gruszka D, Christodoulou V, Davis SJ, von Korff M, Laurie DA (2012) Mutation at the circadian clock gene EARLY MATURITY 8 adapts domesticated barley (*Hordeum vulgare*) to short growing seasons. Proc Natl Acad Sci USA **109**: 8328–8333

González FG, Slafer GA, Miralles DJ (2002) Vernalization and photoperiod responses in wheat pre-flowering reproductive phases. Field Crops Res **74**: 183–195

Goto K, Meyerowitz EM (1994) Function and regulation of the Arabidopsis floral homeotic gene PISTILLATA. Genes Dev **8**: 1548–1560

Gou J, Fu C, Liu S, Tang C, Debnath S, Flanagan A, Ge Y, Tang Y, Jiang Q, Larson PR, (2017) The miR156-SPL4 module predominantly regulates aerial axillary bud formation and controls shoot architecture. New Phytol **216**: 829–840

Griffiths FEW, Lyndon RF, Bennett MD (1985) The effects of vernalization on the growth of the wheat shoot apex. Ann Bot **56**: 501–511

Halliwell J, Borrill P, Gordon A, Kowalczyk R, Pagano ML, Saccomanno B, Bentley AR, Uauy C, Cockram J (2016) Systematic investigation of FLOWERING LOCUS T-like Poaceae gene families identifies the short-day expressed flowering pathway gene, TaFT3 in wheat (*Triticum aestivum* L.). Front Plant Sci **7**: 857

Hartmann U, Höhmann S, Nettesheim K, Wisman E, Saedler H, Huijser P (2000) Molecular cloning of SVP: a negative regulator of the floral transition in Arabidopsis. Plant J **21**: 351–360

Hayama R, Yokoi S, Tamaki S, Yano M, Shimamoto K (2003) Adaptation of photoperiodic control pathways produces short-day flowering in rice. Nature **422**: 719–722

Hemming MN, Peacock WJ, Dennis ES, Trevaskis B (2008) Low-temperature and daylength cues are integrated to regulate FLOWERING LOCUS T in barley. Plant Physiol **147**: 355–366

Hemming MN, Fieg S, Peacock WJ, Dennis ES, Trevaskis B (2009) Regions associated with repression of the barley (Hordeum vulgare) VERNALIZATION1 gene are not required for cold induction. Mol Genet Genomics **282**: 107–117

Hsu CY, Adams JP, Kim H, No K, Ma C, Strauss SH, Drnevich J, Vandervelde L, Ellis JD, Rice BM, (2011) FLOWERING LOCUS T duplication coordinates reproductive and vegetative growth in perennial poplar. Proc Natl Acad Sci USA **108**: 10756–10761

Huang Z, Shi T, Zheng B, Yumul RE, Liu X, You C, Gao Z, Xiao L, Chen X (2017) *APETALA2* antagonizes the transcriptional activity of *AGAMOUS* in regulating floral stem cells in *Arabidopsis thaliana*. New Phytol **215**: 1197–1209

Hyun Y, Lee I (2006) *KIDARI*, encoding a non-DNA Binding bHLH protein, represses light signal transduction in *Arabidopsis thaliana*. Plant Mol Biol **61**: 283–296

Hyun Y, Richter R, Coupland G (2017) Competence to flower: age-controlled sensitivity to environmental cues. Plant Physiol **173**: 36–46

Ikeda K, Ito M, Nagasawa N, Kyozuka J, Nagato Y (2007) Rice ABERRANT PANICLE ORGANIZATION 1, encoding an F-box protein, regulates meristem fate. Plant J **51**: 1030–1040

Jones H, Leigh FJ, Mackay I, Bower MA, Smith LMJ, Charles MP, Jones G, Jones MK, Brown TA, Powell W (2008) Population-based resequencing reveals that the flowering time adaptation of cultivated barley originated east of the Fertile Crescent. Mol Biol Evol **25**: 2211–2219

Jung JH, Seo YH, Seo PJ, Reyes JL, Yun J, Chua NH, Park CM (2007) The GIGANTEA-regulated microRNA172 mediates photoperiodic flowering independent of CONSTANS in Arabidopsis. Plant Cell **19**: 2736–2748

Kardailsky I, Shukla VK, Ahn JH, Dagenais N, Christensen SK, Nguyen JT, Chory J, Harrison MJ, Weigel D (1999) Activation tagging of the floral inducer FT. Science **286**: 1962–1965

Kikuchi R, Kawahigashi H, Ando T, Tonooka T, Handa H (2009) Molecular and functional characterization of PEBP genes in barley reveal the diversification of their roles in flowering. Plant Physiol **149**: 1341–1353

Kobayashi Y, Kaya H, Goto K, Iwabuchi M, Araki T (1999) A pair of related genes with antagonistic roles in mediating flowering signals. Science **286**: 1960–1962

Kojima S, Takahashi Y, Kobayashi Y, Monna L, Sasaki T, Araki T, Yano M (2002) Hd3a, a rice ortholog of the Arabidopsis FT gene, promotes transition to flowering downstream of Hd1 under short-day conditions. Plant Cell Physiol **43**: 1096–1105

Komatsuda T, Pourkheirandish M, He C, Azhaguvel P, Kanamori H, Perovic D, Stein N, Graner A, Wicker T, Tagiri A, (2007) Six-rowed barley originated from a mutation in a homeodomain-leucine zipper I-class homeobox gene. Proc Natl Acad Sci USA **104**: 1424–1429

Komiya R, Ikegami A, Tamaki S, Yokoi S, Shimamoto K (2008) Hd3a and RFT1 are essential for flowering in rice. Development **135**: 767–774

Komiya R, Yokoi S, Shimamoto K (2009) A gene network for long-day flowering activates RFT1 encoding a mobile flowering signal in rice. Development **136**: 3443–3450

Koppolu R, Anwar N, Sakuma S, Tagiri A, Lundqvist U, Pourkheirandish M, Rutten T, Seiler C, Himmelbach A, Ariyadasa R, (2013) Six-rowed spike4 (Vrs4) controls spikelet determinacy and row-type in barley. Proc Natl Acad Sci USA **110**: 13198–13203

Krizek BA (2011) Auxin regulation of Arabidopsis flower development involves members of the AINTEGUMENTA-LIKE/PLETHORA (AIL/PLT) family. J Exp Bot **62**: 3311–3319

Laurie DA (1997) Comparative genetics of flowering time. *In* **T Sasaki and G Moore**, eds, Oryza: From Molecule to Plant. Springer, Dordrecht, Germany, pp 167–177

Laurie DA, Pratchett N, Snape JW, Bezant JH (1995) RFLP mapping of five major genes and eight quantitative trait loci controlling flowering time in a winter x spring barley (Hordeum vulgare L.) cross. Genome **38**: 575–585

Lee JH, Yoo SJ, Park SH, Hwang I, Lee JS, Ahn JH (2007) Role of SVP in the control of flowering time by ambient temperature in Arabidopsis. Genes Dev **21**: 397–402

Li D, Liu C, Shen L, Wu Y, Chen H, Robertson M, Helliwell CA, Ito T, Meyerowitz E, Yu H (2008) A repressor complex governs the integration of flowering signals in Arabidopsis. Dev Cell **15**: 110–120

Licausi F, Ohme-Takagi M, Perata P (2013) APETALA2/Ethylene Responsive Factor (AP2/ERF) transcription factors: mediators of stress responses and developmental programs. New Phytol **199**: 639–649

Lv B, Nitcher R, Han X, Wang S, Ni F, Li K, Pearce S, Wu J, Dubcovsky J, Fu D (2014) Characterization of FLOWERING LOCUS T1 (FT1) gene in Brachypodium and wheat. PLoS One **9**: e94171 24718312

Mandel MA, Gustafson-Brown C, Savidge B, Yanofsky MF (1992) Molecular characterization of the Arabidopsis floral homeotic gene APETALA1. Nature **360**: 273–277

Mascher M, Jost M, Kuon JE, Himmelbach A, Aßfalg A, Beier S, Scholz U, Graner A, Stein N (2014) Mapping-by-sequencing accelerates forward genetics in barley. Genome Biol **15**: R78

Mascher M, Gundlach H, Himmelbach A, Beier S, Twardziok SO, Wicker T, Radchuk V, Dockter C, Hedley PE, Russell J, (2017) A chromosome conformation capture ordered sequence of the barley genome. Nature **544**: 427–433

Matthews PR, Wang MB, Waterhouse PM, Thornton S, Fieg SJ, Gubler F, Jacobsen JV (2001) Marker gene elimination from transgenic barley, using co-transformation with adjacent twin T-DNAs' on a standard Agrobacterium transformation vector. Mol Breed **7**: 195–202

McKinney HH, Sando WJ (1935) Earliness of sexual reproduction in wheat as influenced by temperature and light in relation to growth phases. J Agric Res **51**: 621–641

Michaels SD, Himelblau E, Kim SY, Schomburg FM, Amasino RM (2005) Integration of flowering signals in winter-annual Arabidopsis. Plant Physiol **137**: 149–156

Miralles DJ, Richards RA (2000) Response of leaf and tiller emergence and primordium initiation in wheat and barley to interchanged photoperiod. Ann Bot **85**: 655–663

Miyoshi K, Ahn B-O, Kawakatsu T, Ito Y, Itoh J-I, Nagato Y, Kurata N (2004) PLASTOCHRON1, a timekeeper of leaf initiation in rice, encodes cytochrome P450. Proc Natl Acad Sci USA **101**: 875–880

Mouradov A, Cremer F, Coupland G (2002) Control of flowering time: interacting pathways as a basis for diversity. Plant Cell 14 (Suppl): S111–S130

Mulki MA, von Korff M (2016) CONSTANS controls floral repression by up-regulating VERNALIZATION2 (VRN-H2) in Barley. Plant Physiol **170**: 325–337

Pankin A, Campoli C, Dong X, Kilian B, Sharma R, Himmelbach A, Saini R, Davis SJ, Stein N, Schneeberger K, (2014) Mapping-by-sequencing identifies HvPHYTOCHROME C as a candidate gene for the early maturity 5 locus modulating the circadian clock and photoperiodic flowering in barley. Genetics **198**: 383–396

Patro R, Duggal G, Love MI, Irizarry RA, Kingsford C (2017) Salmon provides fast and bias-aware quantification of transcript expression. Nat Methods **14**: 417–419

Pearce S, Vanzetti LS, Dubcovsky J (2013) Exogenous gibberellins induce wheat spike development under short days only in the presence of VERNALIZATION1. Plant Physiol **163**: 1433–1445 24085801

Pelaz S, Ditta GS, Baumann E, Wisman E, Yanofsky MF (2000) B and C floral organ identity functions require SEPALLATA MADS-box genes. Nature **405**: 200–203

Ramsay L, Comadran J, Druka A, Marshall DF, Thomas wild-type, Macaulay M, MacKenzie K, Simpson C, Fuller J, Bonar N, (2011) INTERMEDIUM-C, a modifier of lateral spikelet fertility in barley, is an ortholog of the maize domestication gene TEOSINTE BRANCHED 1. Nat Genet **43**: 169–172

Ritchie ME, Phipson B, Wu D, Hu Y, Law CW, Shi W, Smyth GK (2015) limma powers differential expression analyses for RNA-sequencing and microarray studies. Nucleic Acids Res **43**: e47

Roberts EH, Summerfield RJ, Cooper JP, Ellis RH (1988) Environmental control of flowering in barley (*Hordeum vulgare* L.). I. Photoperiod limits to long-day responses, photoperiod-insensitive phase and effects of low-temperature and short-day vernalization. Ann Bot **62**: 127–144

Rollins JA, Drosse B, Mulki MA, Grando S, Baum M, Singh M, Ceccarelli S, von Korff M (2013) Variation at the vernalisation genes Vrn-H1 and Vrn-H2 determines growth and yield stability in barley (*Hordeum vulgare*) grown under dryland conditions in Syria. Theor Appl Genet **126**: 2803–2824

Sakamoto T, Kobayashi M, Itoh H, Tagiri A, Kayano T, Tanaka H, Iwahori S, Matsuoka M (2001) Expression of a gibberellin 2-oxidase gene around the shoot apex is related to phase transition in rice. Plant Physiol **125**: 1508–1516

Sasani S, Hemming MN, Oliver SN, Greenup A, Tavakkol-Afshari R, Mahfoozi S, Poustini K, Sharifi HR, Dennis ES, Peacock WJ, (2009) The influence of vernalization and daylength on expression of flowering-time genes in the shoot apex and leaves of barley (*Hordeum vulgare*). J Exp Bot **60**: 2169–2178

Sawers RJ, Linley PJ, Gutierrez-Marcos JF, Delli-Bovi T, Farmer PR, Kohchi T, Terry MJ, Brutnell TP (2004) The Elm1 (ZmHy2) gene of maize encodes a phytochromobilin synthase. Plant Physiol **136**: 2771–2781

Schmid M, Uhlenhaut NH, Godard F, Demar M, Bressan R, Weigel D, Lohmann JU (2003) Dissection of floral induction pathways using global expression analysis. Development **130**: 6001–6012

Schwarz S, Grande AV, Bujdoso N, Saedler H, Huijser P (2008) The microRNA regulated SBP-box genes SPL9 and SPL15 control shoot maturation in Arabidopsis. Plant Mol Biol **67**: 183–195

Shimada S, Ogawa T, Kitagawa S, Suzuki T, Ikari C, Shitsukawa N, Abe T, Kawahigashi H, Kikuchi R, Handa H, (2009) A genetic network of flowering-time genes in wheat leaves, in which an APETALA1/FRUITFULL-like gene, VRN1, is upstream of FLOWERING LOCUS T. Plant J **58**: 668–681

Simpson GG, Dean C (2002) Arabidopsis, the Rosetta stone of flowering time? Science **296**: 285–289

Slafer GA, Rawson HM (1994) Sensitivity of wheat phasic development to major environmental factors: a re-examination of some assumptions made by physiologists and modellers. Funct Plant Biol **21**: 393–426

Tingay S, McElroy E, Kalla R, Fieg S, Wang M, Thornton S, Brettell R (1997) *Agrobacterium tumefaciens*-mediated barley transformation. Plant J **11**: 1369–1376

Torti S, Fornara F, Vincent C, Andrés F, Nordström K, Göbel U, Knoll D, Schoof H, Coupland G (2012) Analysis of the Arabidopsis shoot meristem transcriptome during floral transition identifies distinct regulatory patterns and a leucine-rich repeat protein that promotes flowering. Plant Cell **24**: 444–462

Turner A, Beales J, Faure S, Dunford RP, Laurie DA (2005) The pseudo-response regulator Ppd-H1 provides adaptation to photoperiod in barley. Science **310**: 1031–1034

van Esse GW, Walla A, Finke A, Koornneef M, Pecinka A, von Korff M (2017) Six-rowed Spike3 (VRS3) is a histone demethylase that controls lateral spikelet development in barley. Plant Physiol **174**: 2397–2408

von Korff M, Wang H, Léon J, Pillen K (2006) AB-QTL analysis in spring barley: II. Detection of favourable exotic alleles for agronomic traits introgressed from wild barley (*H. vulgare* ssp. spontaneum). Theor Appl Genet **112**: 1221–1231

von Korff M, Léon J, Pillen K (2010) Detection of epistatic interactions between exotic alleles introgressed from wild barley (*H. vulgare* ssp. spontaneum). Theor Appl Genet **121**: 1455–1464

Waddington SR, Cartwright PM, Wall PC (1983) A quantitative scale of spike initial and pistil development in barley and wheat. Ann Bot **51**: 119–130

Wang H, Wang H (2015) Multifaceted roles of FHY3 and FAR1 in light signaling and beyond. Trends Plant Sci **20**: 453–461

Wang G, Schmalenbach I, von Korff M, Léon J, Kilian B, Rode J, Pillen K (2010) Association of barley photoperiod and vernalization genes with QTLs for flowering time and agronomic traits in a BC2DH population and a set of wild barley introgression lines. Theor Appl Genet **120**: 1559–1574

Wang JW, Czech B, Weigel D (2009) miR156-regulated SPL transcription factors define an endogenous flowering pathway in Arabidopsis thaliana. Cell **138**: 738–749

Wang MB, Matthews PR, Upadhyaya NM, Waterhouse PM (1998) Improved vectors for Agrobacterium tumefaciens-mediated transformation of monocot plants. Acta Hortic **461**: 401–407

Wigge PA, Kim MC, Jaeger KE, Busch W, Schmid M, Lohmann JU, Weigel D (2005) Integration of spatial and temporal information during floral induction in Arabidopsis. Science **309**: 1056–1059

Yamaguchi A, Wu MF, Yang L, Wu G, Poethig RS, Wagner D (2009) The microRNA-regulated SBP-Box transcription factor SPL3 is a direct upstream activator of LEAFY, FRUITFULL, and APETALA1. Dev Cell **17**: 268–278

Yan L, Loukoianov A, Tranquilli G, Helguera M, Fahima T, Dubcovsky J (2003) Positional cloning of the wheat vernalization gene VRN1. Proc Natl Acad Sci USA **100**: 6263–6268

Yan L, Loukoianov A, Blechl A, Tranquilli G, Ramakrishna W, SanMiguel P, Bennetzen JL, Echenique V, Dubcovsky J (2004) The wheat VRN2 gene is a flowering repressor down-regulated by vernalization. Science **303**: 1640–1644

Yan L, Fu D, Li C, Blechl A, Tranquilli G, Bonafede M, Sanchez A, Valarik M, Yasuda S, Dubcovsky J (2006) The wheat and barley vernalization gene VRN3 is an orthologue of FT. Proc Natl Acad Sci USA **103**: 19581–19586

Yant L, Mathieu J, Dinh TT, Ott F, Lanz C, Wollmann H, Chen X, Schmid M (2010) Orchestration of the floral transition and floral development in Arabidopsis by the bifunctional transcription factor APETALA2. Plant Cell **22**: 2156–2170

Yoo SK, Chung KS, Kim J, Lee JH, Hong SM, Yoo SJ, Yoo SY, Lee JS, Ahn JH (2005) *CONSTANS* activates *SUPPRESSOR OF OVEREXPRESSION OF CONSTANS 1* through *FLOWERING LOCUS T* to promote flowering in *Arabidopsis*. Plant Physiol **139**: 770–778

Zadoks JC, Chang TT, Konzak CF (1974) A decimal code for the growth stages of cereals. Weed Res **14**: 415–421